

Borders and Cytoarchitecture of the Perirhinal and Postrhinal Cortices in the Rat

REBECCA D. BURWELL*

Department of Psychology, Brown University, Providence, Rhode Island 02912

ABSTRACT

Cytoarchitectonic and histochemical analyses were carried out for perirhinal areas 35 and 36 and the postrhinal cortex, providing the first detailed cytoarchitectonic study of these regions in the rat brain. The rostral perirhinal border with insular cortex is at the extreme caudal limit of the claustrum, consistent with classical definitions of insular cortex dating back to Rose ([1928] *J. Psychol. Neurol.* 37:467–624). The border between the perirhinal and postrhinal cortices is at the caudal limit of the angular bundle, as previously proposed by Burwell et al. ([1995] *Hippocampus* 5:390–408). The ventral borders with entorhinal cortex are consistent with the Insausti et al. ([1997] *Hippocampus* 7:146–183) description of that region and the Dolorfo and Amaral ([1998] *J. Comp. Neurol.* 398:25–48) connectional findings. Regarding the remaining borders, both the perirhinal and postrhinal cortices encroach upon temporal cortical regions as defined by others (e.g., Zilles [1990] *The cerebral cortex of the rat*, p 77–112; Paxinos and Watson [1998] *The rat brain in stereotaxic coordinates*). Based on cytoarchitectonic and histochemical criteria, perirhinal areas 35 and 36 and the postrhinal cortex were further subdivided. Area 36 was parceled into three subregions, areas 36d, 36v, and 36p. Area 35 was parceled into two cytoarchitectonically distinctive subregions, areas 35d and 35v. The postrhinal cortex was divided into two subregions, areas PORd and PORv. These regional definitions of perirhinal areas 35 and 36 and the postrhinal cortex were confirmed by new empirical analyses of previously reported quantitative connectional data (Burwell and Amaral [1998a] *J. Comp. Neurol.* 398:179–205). *J. Comp. Neurol.* 437:17–41, 2001. © 2001 Wiley-Liss, Inc.

Indexing terms: polysensory cortex; hippocampus; memory; parahippocampal

In recent years the function of higher order polymodal associational regions has come under increasing scrutiny, especially in the areas of research on the neural basis of learning and memory. Two regions receiving particular emphasis, the perirhinal cortex and the postrhinal cortex (parahippocampal in the monkey), are especially interesting for their strong reciprocal connectivity with the entorhinal cortex and with structures within the hippocampal formation including the hippocampus proper and the subiculum (Deacon et al., 1983; Burwell and Amaral, 1998b; Naber et al., 1999).

The perirhinal and postrhinal cortices are distinguished from each other by a number of connectional features. For example, they exhibit different terminal projection patterns to the entorhinal cortex (Deacon et al., 1983; Burwell and Amaral, 1998b). Both regions can be described as polymodal associational cortex, i.e., they receive unimodal input from more than one sensory modality as well as input from other polymodal associational regions. With

respect to cortical connectivity, both regions receive substantial input from higher order associational regions, the perirhinal cortex from more anterior associational regions and the postrhinal cortex from more posterior associational regions. Regarding unimodal input, the perirhinal cortex receives input from all sensory modalities, whereas the postrhinal cortex is preferentially innervated by visual and visuospatial regions (Burwell and Amaral, 1998a).

These patterns of cortical afferentation suggest that the perirhinal and postrhinal cortices participate in different ways in the integration of polymodal sensory information.

Grant sponsor: NIH; Grant number: MH57268-R03; Grant sponsor: NSF; Grant number: IBN-9875792.

*Correspondence to: Rebecca D. Burwell, Brown University Department of Psychology, 89 Waterman St., Providence, RI 02912.
E-mail: Rebecca_Burwell@Brown.edu

Received 12 May 2000; Revised 11 May 2001; Accepted 15 May 2001

What is known about the subcortical connections of these regions is consistent with that view. The perirhinal cortex exhibits strong connectivity with multiple nuclei of the amygdaloid complex, suggesting a role in reward learning (McDonald and Jackson, 1987; McDonald, 1998; Shammah-Lagnado et al., 1999; Shi and Cassell, 1999; Pitkanen et al., 2000). In contrast, the postrhinal connections to the amygdala, although present, appear to be weaker and limited to the lateral and accessory basal nuclei of the amygdala (reviewed in McDonald, 1998; Pitkanen et al., 2000). Other studies have provided information about the thalamic connectivity of the perirhinal cortex, which is more distributed than that of unimodal cortical areas (Krettek and Price, 1977a; Moga et al., 1995; Aggleton and Brown, 1999; Rudiger, 1999; Van Groen et al., 1999). Although less is known about the thalamic connections of the postrhinal cortex, there does appear to be a substantial input from the lateral posterior nucleus of the thalamus (Deacon et al., 1983; Burwell et al., 1995; Chen and Burwell, 1996; Shi and Cassell, 1997), suggesting a possible role in visuospatial attention.

Numerous neuroanatomical and functional studies of the rat perirhinal cortex have been carried out in recent years, but research has been hampered by the absence of cytoarchitectonic descriptions of the regions in question. At the same time, the borders for perirhinal cortex in the rat have differed among investigators, and, until recently, there was no region that was considered the homologue to the parahippocampal cortex in the monkey. The differing historical descriptions have been reviewed in detail earlier (Burwell et al., 1995) and so are only briefly discussed and illustrated here (Fig. 1). The major discrepancies fall into three categories. First, neuroanatomists have differed with respect to the number of regions and subregions into which these cortical areas should be divided. Rose and Krieg both defined two regions associated with the posterior rhinal sulcus in the rodent brain corresponding to areas 35 and 36. A number of recent descriptions have followed suit (but see Zilles, 1985; Paxinos and Watson, 1998; Swanson, 1998). Others have proposed that cortex associated with the posterior half of the rhinal sulcus in

the rat could be divided on cytoarchitectural and connective criteria into a rostral region, the perirhinal cortex, and a caudal region, the postrhinal cortex (Deacon et al., 1983; Burwell et al., 1995; Burwell, 2000).

Second, there has been little agreement on the dorsal borders, with nearly every map of cortical areas in the rodent brain defining the border between perirhinal cortex and the remaining temporal cortex differently (Brodman, 1909; Rose, 1929; Krieg, 1946a; Zilles, 1985; Schober, 1986; Paxinos and Watson, 1998; Swanson, 1998). Even the dorsal boundaries of the recently defined postrhinal cortex have varied (compare Burwell et al., 1995 with Witter et al., 2000).

Finally, the placement of the rostral border of perirhinal cortex with insular regions is somewhat controversial. An early description by Rose (1929) placed the border of the perirhinal cortex with the insular cortex at the caudal limit of the claustrum (Fig. 1A). Other investigators have not felt constrained to adhere to this classical definition and thus moved the border caudally by various distances (e.g., Krieg, 1946a; McDonald, 1998; Shi and Cassell, 1998). Although in Krieg (1946a) the justification for revision is unclear, others assert that the unimodal input to the rostral perirhinal cortex is exclusively somatosensory and that the region is thus more appropriately considered insular cortex (Fabri and Burton, 1991; McDonald, 1998; Shi and Cassell, 1998; but see Burwell and Amaral, 1998a).

Burwell et al. (1995) attempted to address these issues with the information available at the time (Fig. 2). They provided preliminary borders and cytoarchitectonic criteria for the perirhinal cortex (areas 35 and 36) and defined the region dorsally adjacent to the posterior extent of the rhinal sulcus as postrhinal cortex. Those definitions adhered in several ways to the early definition provided by Rose (1929) in that perirhinal cortex arose at the caudal limit of the claustrum and was divided into two subregions. The terminology, however, was taken from Brodman (1909) and Krieg (1946b) in an effort to maintain consistency with the monkey model and to facilitate comparative analyses. Thus, perirhinal cortex was defined as

Abbreviations

| | | | |
|-----------|--|-------|---|
| AId | agranular insular area, dorsal part | PORv | postrhinal cortex, ventral part |
| AIp | agranular insular area, posterior part | RSPd | retrosplenial area, dorsal part |
| AIV | agranular insular area, ventral part | RSPv | retrosplenial area, ventral part |
| AUDp | primary auditory area | SPRSQ | semi partial R-squared |
| AUDv | ventral auditory area | SSp | primary somatosensory cortical area |
| CA1, CA2, | | SSs | secondary somatosensory cortical area |
| CA3 | CA fields of the hippocampus | rs | rhinal sulcus |
| DY | Diamidino yellow | TCS | tissue collecting solution |
| Ent | entorhinal cortex | TeA | temporal association cortex |
| Entl | entorhinal area, lateral part | TeV | ventral temporal association cortex |
| Entm | entorhinal area, medial part | TF | area TF of the primate parahippocampal cortex |
| FB | Fast blue | TH | area TH of the primate parahippocampal cortex |
| FG | Fluoro-Gold | VISC | visceral area |
| GI | granular insular cortex | VISl | lateral visual areas |
| GU | gustatory area | VISm | medial visual areas |
| ORB1 | orbital area, lateral part | VISp | primary visual area |
| ORBm | orbital area, medial part | 35 | perirhinal area 35 |
| ORBvl | orbital area, ventrolateral part | 35d | perirhinal area 35, dorsal part |
| PaSub | parasubiculum | 35v | perirhinal area 35, ventral part |
| PIR | piriform area | 36 | perirhinal area 36 |
| PER | perirhinal cortex | 36d | perirhinal area 36, dorsal part |
| POR | postrhinal cortex | 36v | perirhinal area 36, ventral part |
| PORd | postrhinal cortex, dorsal part | | |

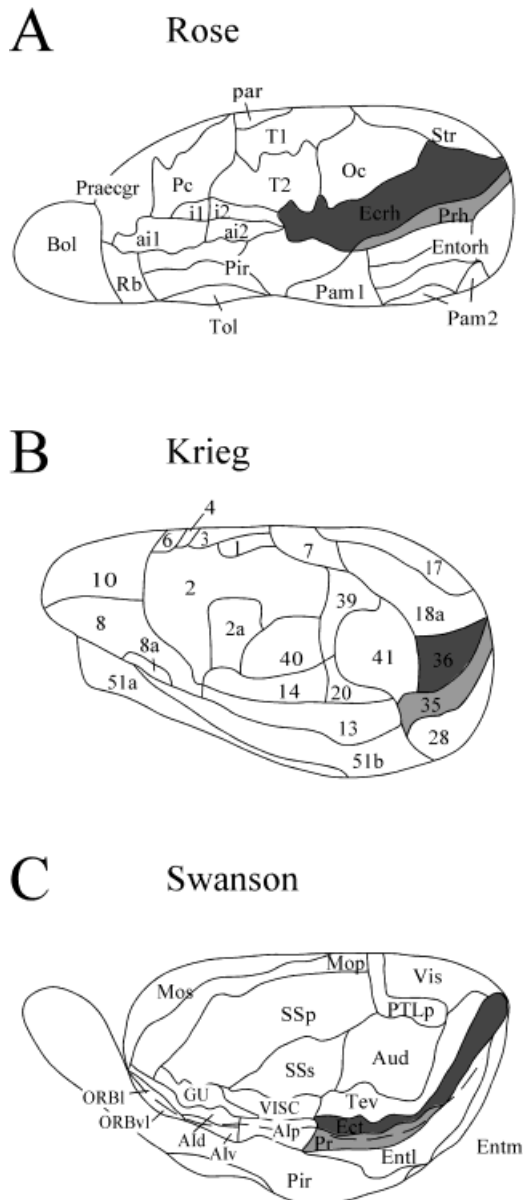


Fig. 1. Regional definitions of the cortical mantle for the rat brain. For each map, the region comparable to area 36 is shown in dark gray and the region comparable to area 35 is shown in light gray. Surface views of the mouse brain adapted from Rose (1929) (A) and the rat brain adapted from Krieg (1946a) (B) and Swanson (1998) (C). Taken together, these views illustrate the controversy historically surrounding the definition and nomenclature of the perirhinal cortex in the rodent brain. Relevant abbreviations: Ecrh or Ec, ectorhinal cortex; Prh, perirhinal cortex; PRr and PRc, rostral and caudal perirhinal cortex; POR, postrhinal cortex.

comprising areas 35 and 36. Based on cytoarchitectonic and connectional criteria, Burwell et al. (1995) parceled out the caudal portion of the region and followed Deacon et al. (1983) in terming that area the postrhinal cortex, although its borders do not conform to those of Deacon et al. (1983). Subsequent anterograde and retrograde connectional studies used those preliminary borders to examine in detail the organization of the perirhinal and postrhinal

intrinsic connections and their connections with the entorhinal cortex (Burwell and Amaral, 1998b) and to quantify the neocortical afferentation of the perirhinal, postrhinal, and entorhinal cortices (Burwell and Amaral, 1998a). Those findings provided important connectional criteria for the present study.

Despite the neuroanatomical and other studies mentioned above and the recent numerous functional studies of the perirhinal cortex (e.g., Aggleton et al., 1997; Otto et al., 1997; Zhu et al., 1997; Liu and Bilkey, 1998; Wiig and Burwell, 1998; Bucci et al., 2000; Vann et al., 2000), there is a surprising lack of detailed descriptions of the structure of these regions. Krieg (1946b) contributed a paragraph or two each for areas 35 and 36. Rose (1928) provided detailed analyses of the rostrally adjacent insular cortex for several rodent species, not including the rat, but no one has contributed an equally detailed description of the rodent perirhinal cortex. Moreover, a cytoarchitectonic study of the postrhinal cortex is entirely lacking. Thus, the present study was undertaken to provide a thorough cytoarchitectonic analysis of the perirhinal and postrhinal cortices of the rat and to provide structural criteria for borders based on cytoarchitectonic, myeloarchitectonic, and histochemical criteria informed by connectional findings.

MATERIALS AND METHODS

Subjects

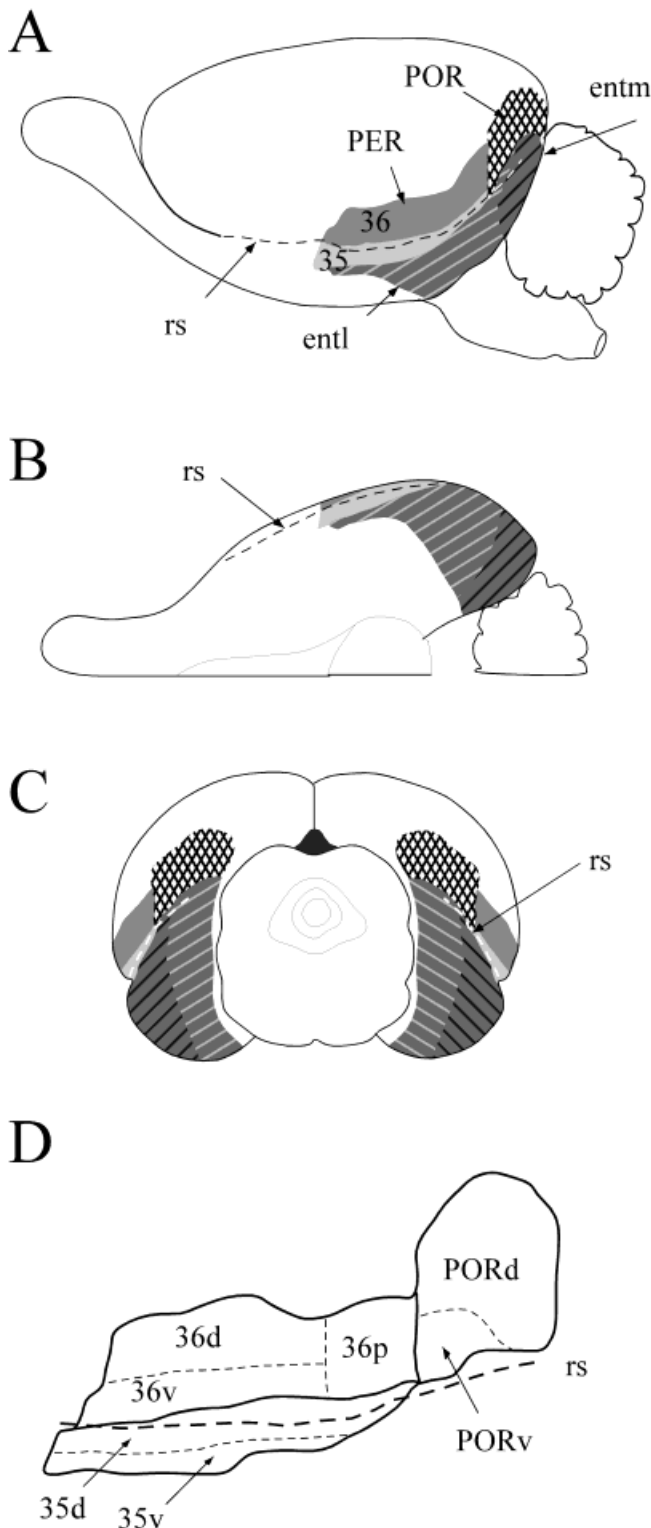
Six brains were especially prepared for this study to permit processing for a selected set of histo- and cytochemical stains. In order to select the most informative preparations, 13 archival cases were also consulted. The primary subjects were previously untreated adult male Sprague-Dawley rats (Charles River Laboratories, Raleigh, NC) weighing between 250 and 350 g. Archival subjects were previously untreated adult male Sprague-Dawley rats obtained from Harlan Laboratories (Houston, TX). All methods involving the use of live subjects were approved by the appropriate institutional animal care committee and conformed to NIH guidelines.

Tissue processing

Subjects were deeply anesthetized with Nembutal (50 mg/kg, i.p.). The subjects were transcardially perfused with a peristaltic pump at a flow rate of 35–40 ml/min. For cases that would be processed for heavy metals, rats were perfused according to a method adapted from Sloviter (1982) through the ascending aorta with a 0.37% sulphide solution (pH 7.2) for 5 minutes followed by an additional 15-minute perfusion with 10% neutral buffered formalin (pH 7.2). For cases in which sulphide perfusion was unnecessary, room temperature saline was first perfused for 2 minutes to clear the blood. Saline was followed by a solution of 4% paraformaldehyde in 0.1 M sodium phosphate buffer (pH 7.4) at 4°C for 15 minutes. Ice was packed around the head of the animals during perfusion. After removal from the skull, the brains were cryoprotected for 24 hours by placement in 20% glycerol in 0.1 M sodium phosphate buffer (pH 7.4) at 4°C.

The brains were coronally sectioned at 30 or 40 μ m on a freezing microtome. Sections were collected in five series for processing and storage. Depending on the experiment, one or two series were collected in sodium phosphate

buffer (pH 7.4) for immunohistochemical processing. One or two series were stored in formalin for later processing using cell and myelin stains. One or two series were stored at -20°C in cryoprotectant TCS consisting of 30% ethylene glycol and 20% glycerol in sodium phosphate buffer (pH 7.4).



Histochemical procedures

In order to select the most informative preparations, 13 archival cases were consulted. These were cut in the coronal, horizontal, or sagittal plane and stained for some combination of Nissl, myelin, acetylcholinesterase, choline acetyltransferase, parvalbumin, and/or nonphosphorylated neurofilament protein (with the antibody SMI-32). Examination of the archival material indicated that several markers provided a clear border between the entorhinal and perirhinal cortex. These included immunohistochemical staining for parvalbumin and nonphosphorylated neurofilament protein as well as Timm's histochemical method of staining for heavy metals. Material prepared using Timm's method also provided useful distinguishing features for both area 35 and area 36 and for the adjacent cortical regions. Preparations stained for choline acetyltransferase were not very useful for distinguishing the target regions from one another or from adjacent cortices. Staining for acetylcholinesterase was useful primarily for identifying subcortical landmarks. Thus, Timm's method was chosen to complement the traditional cell-stained and myelin-stained preparations.

Brains were prepared such that a series of neuroanatomical markers could be examined in adjacent sections. The brain used for documentation in the present report was sectioned in the coronal plane and processed for Nissl, fiber, acetylcholinesterase, and heavy metals.

Nissl and fiber stain

After storage in 10% formalin solution for at least 3 days, one series was rinsed in phosphate buffer (pH 7.4) and mounted on glass slides. After drying in a 40°C oven at least overnight, slides destined for Nissl stain were defatted in a solution of equal parts chloroform and ethanol and hydrated in a descending series of alcohol solutions. The sections were stained using a 0.25% thionin solution and differentiated in a dilute solution of glacial acetic acid in 95% ethanol (about 4 drops in 250 mls). Following thionin staining, slides were dehydrated in an ascending series of alcohols, incubated 3×3 minutes in xylene, and coverslipped by using DPX mountant (BDH Laboratory Supplies, Poole, England). Adjacent sections were stained for myelinated fibers by the Quinn and Graybiel (1994) adaptation of the Schmued (1990) protocol. This is a gold chloride staining procedure that is safer and more reliable than the traditional Gallyas technique. Free-floating sections were rinsed in phosphate-buffered saline (pH 7.4) prior to beginning the staining procedure. A buffered saline solution (pH 7.4) was used as a vehicle for the gold chloride. The Quinn and Graybiel modification uses trace amounts of hydrogen peroxide in the gold chloride solution, which increases the reliability of the technique. After staining in gold chloride, tissue was fixed in a

Fig. 2. Lateral (A), ventral (B), and caudal (C) surface views of the rat brain illustrating the locations of the perirhinal, postrhinal, and entorhinal cortices. The perirhinal cortex (PER) is shown in gray, area 36 in dark gray, and area 35 in light gray. The postrhinal cortex (POR) is shown with a cross-hatched pattern. The entorhinal cortex is shown in gray with diagonal stripes, dark stripes for the medial entorhinal area (Entm) and light for the lateral entorhinal area (Entl). D: Unfolded map of the perirhinal and postrhinal cortices showing regional and subdivisional borders.

5% sodium thiosulfate solution. Sections were mounted on subbed slides, dried at least overnight in a 40°C oven, dehydrated as for Nissl stain, and coverslipped by using DPX mountant.

Timm's sulphide silver stain

Tissue was sectioned into phosphate buffer (pH 7.4) and mounted on slides immediately or stored in TCS for later processing. The mounted tissue was stained according to Timm's sulphide silver method (Slovitor, 1982). Using acid-washed glassware, a solution of silver nitrate and hydroquinone in citrate buffer (pH 7.2) mixed with 33% gum arabic in distilled H₂O was freshly prepared for developing the slide-mounted material. The slides were processed in a darkroom at 26°C for approximately 30–60 minutes depending on visual assessment of the speed of the reaction. The reaction was stopped when all three sublayers of the dentate gyrus molecular layer were visible. To stop development, slides were washed in running tap water in the dark for 10 minutes and then dipped in distilled H₂O. Slides were then dehydrated in graded alcohols followed by xylene and coverslipped.

Acetylcholinesterase stain

For some cases one series was stained for the demonstration of acetylcholinesterase according to Hedreen et al. (1985). All solutions were prepared in acid-washed glassware. The enzymatic reaction was carried out in polypropylene tissue wells with net bottoms. The tissue was collected and rinsed in a sodium acetate buffer (pH 6.0). The free-floating sections were then incubated in a solution of cupric sulfate, potassium ferrocyanide, and ethopropazine for 30 minutes. After rinsing in sodium acetate buffer, the tissue was washed in 4% ammonium sulfide for one minute. After thorough washing in sodium nitrate buffer (pH 7.2), the tissue was intensified in a silver nitrate solution for 1 minute. The tissue was mounted on gelatin-coated slides within a few days, dried overnight at room temperature, dehydrated in graded alcohols, and coverslipped from xylene by using DPX.

Structural analyses and photomicroscopy

Anatomical preparations were systematically examined at several magnifications, by using traditional neuroanatomical methods of observation. Characteristics of cell morphology, lamination, histochemistry, and fiber architecture were described for different rostrocaudal levels with particular attention to what features provided the most reliable criteria for identifying subregional and regional borders.

For illustration of the cytoarchitectonic, myeloarchitectonic, and histochemical organization of the perirhinal and postrhinal cortices, photomicrographs were taken of coronal sections at nine rostrocaudal levels (Fig. 3) by using a Nikon Optiphot-2 with a Nikon Microflex HFX-DX 35-mm photomicrographic attachment. Black and white negatives were scanned into Adobe Photoshop 5.0 (Adobe Systems, Mountain View, CA) at 2700 dpi by using a Nikon LS-2000 film scanner. The images were enlarged, resulting in a final resolution of at least 500 dpi. Images were then adjusted for brightness and contrast. Composites were constructed in Adobe Photoshop. Text and borders were added in Canvas 7.0 (Deneba Software, Miami FL).

Confirmatory data analyses

Using classification data analysis techniques (Gordon, 1999), previously published empirical cortical afferent data for the perirhinal and postrhinal cortices (Burwell and Amaral, 1998a) were applied to quantitatively address the cytoarchitectural definitions of perirhinal areas 35 and 36 and the postrhinal cortex. The question of interest was whether definition using cytoarchitectonic and histochemical analysis of these cortical regions would correspond to statistical classification based on patterns of cortical afferentation. If the two classifications converged, this would suggest that the connective characteristics of the perirhinal and postrhinal cortices can provide independent confirmation of regional definitions based on traditional neuroanatomical analysis of cytoarchitectonic and other structural characteristics.

The cortical afferent data employed were obtained by plotting retrogradely labeled cells in the entire neocortex for 18 injection sites placed in the perirhinal and postrhinal cortex in the rat (Burwell and Amaral, 1998a). An additional case (116DY) plotted at the same time was quantified for inclusion in the present study because of its particularly informative location. Total numbers and densities were estimated for 29 neocortical areas for each injection site. Cluster analysis was conducted to determine how retrograde tracer injections would be grouped based solely on the pattern of retrogradely labeled cells in the neocortical regions and without information about the neuroanatomical location of the injection sites. The cluster algorithm employed was a hierarchical agglomerative method, Ward's method. This technique is slightly biased toward producing clusters with the same size (SAS, 1996), which would permit further analyses using multivariate approaches. The similarity coefficient was euclidian distance. The cluster solution was chosen by plotting the number of clusters against the semi partial R-squared (SPRSQ) and selecting the number of clusters at which the curve flattened markedly. Such a flattening of the curve is an indication that further division of clusters would have less effect on the amount of variance accounted for by the solution. The cluster analysis was evaluated by using an external validation technique. The cluster solution was statistically compared with classification of injection sites based on neuroanatomical location by using Rand's (1971) statistic (R) such that a value of 0 is obtained when two classifications exhibit no similarity and a value of 1 is obtained when two classifications are identical (see also Hubert and Arabie, 1986).

Two additional analyses were employed: First, the cluster solution was examined by multivariate analysis of variance (MANOVA) to determine what regional inputs significantly distinguished the groupings of injection sites. Second, canonical discriminant analysis was used to determine the magnitude and direction of effects of specific regional input variables upon the groupings of injection sites (Gordon, 1999). The discriminant analysis permitted a graphical presentation of the cortical afferent data that illustrates how clusters of injection sites differ in relation to sources of cortical input.

Nomenclature

Borders for the entorhinal cortex were taken from Insausti et al. (1997) and are consistent with Dolorfo and Amaral (1998). For cortical regions other than the perirhi-

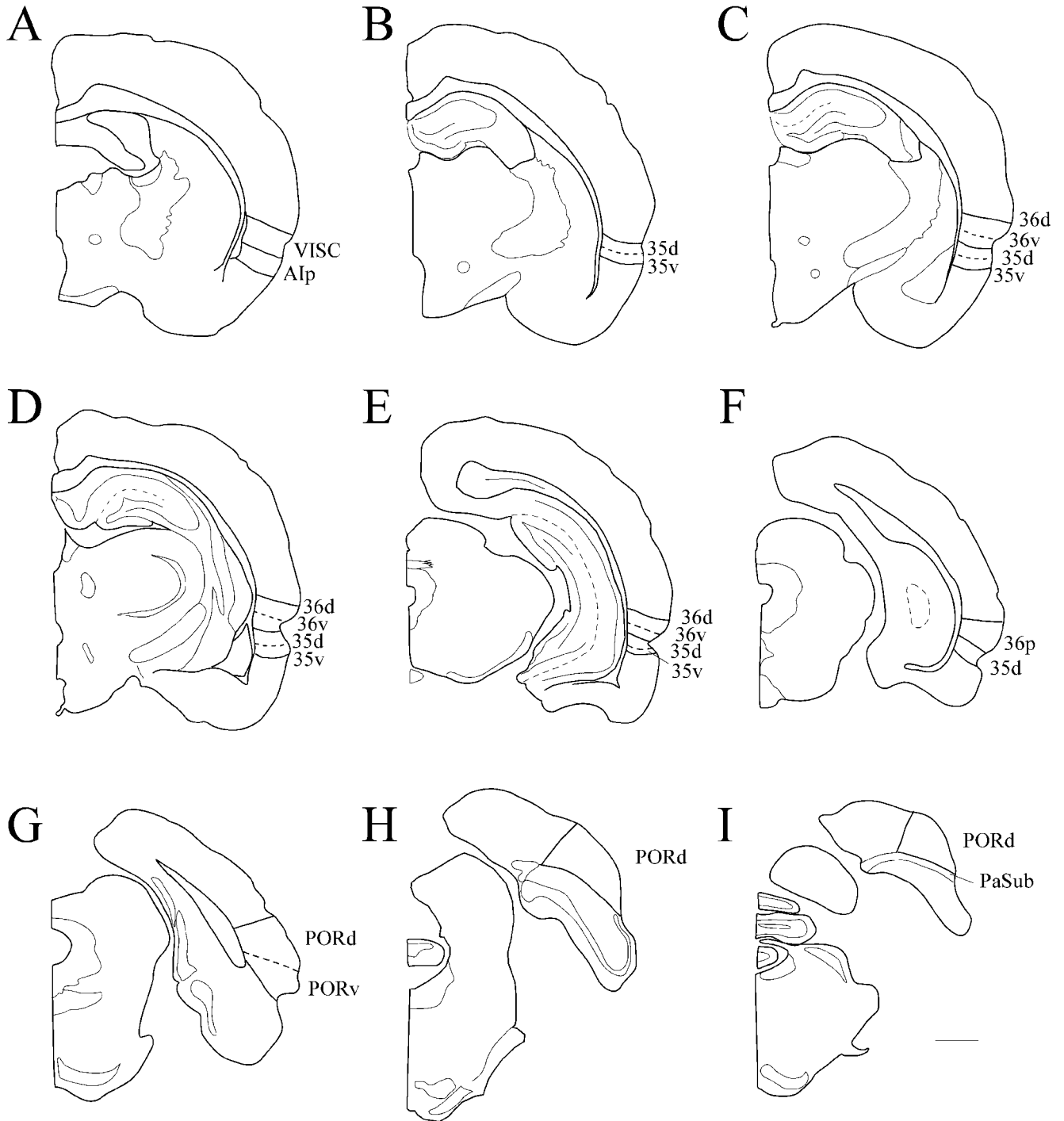


Fig. 3. Schematic showing coronal sections at nine rostrocaudal levels. Each level corresponds to one row of the photomicrographs shown in Figures 4, 7, and 9. Bregma locations according to Paxinos and Watson (1998) are -1.40 mm (A), -2.56 mm (B), -2.80 mm (C), -3.80 mm (D), -5.30 mm (E), -6.72 mm (F), -7.64 mm (G), -8.30 mm (H), and -9.16 mm (I) relative to bregma. Scale bar = 1 mm.

nal, postrhinal, and entorhinal cortices, regional borders and nomenclature conform to those put forth by Swanson (1992, 1998). This resource was chosen first, because the atlas is based on a careful review of the neuroanatomical literature with particular attention to the cytoarchitec-

tonic and connective criteria that were used to delimit each cortical region, and second, because these parcellations have been used previously to analyze experimental data with good success (Wada et al., 1989; Burwell and Amaral, 1998a). In some cases nomenclature was related

to that used in the stereotaxic atlas of Paxinos and Watson (1986, 1998) because this is a commonly used tool in neuroscientific research employing the rat model. Notably, the cortical borders for the recent edition of Paxinos and Watson (1998) are highly similar to those of Swanson (1992, 1998).

In the present account rostrocaudal levels of sections are identified relative to bregma (Paxinos and Watson, 1998). It is known that the use of bregma coordinates is not reliable across sex, age, and strain differences. Thus, it should be noted that rostrocaudal levels of coronal sections belonging to the case illustrated are referenced according to the closest matching plane in Paxinos and Watson (1998) and not relative to the actual location of bregma in the experimental case itself. Thus, a reference to bregma used here is shorthand for referring to landmarks characterizing a rostrocaudal level in the rat brain that corresponds to a plane of section documented in Paxinos and Watson (1998).

RESULTS

Examination of archival cases that included a number of immunohistochemical and histochemical markers suggested that the Timm's method of staining for heavy metals would best complement the traditional cell-stained and myelin-stained preparations used in the present report. Thus, the present account includes cytoarchitectonic, myeloarchitectonic, and histochemical features of perirhinal areas 35 and 36 and the postrhinal cortex. The results of a new confirmatory analysis of previously collected connective data (Burwell and Amaral, 1998a) are also presented.

Perirhinal cortex

The perirhinal cortex comprises two narrow strips of cortex, areas 35 and 36 (Fig. 2), which are adjacent to one another and situated approximately along the third quarter of the rhinal sulcus. Figure 3 shows the coronal levels at which photomicrographs were taken to illustrate structural features of the target regions. Rostrally, the perirhinal cortex includes the fundus of the rhinal sulcus, both banks, and the dorsally adjacent cortex. Moving caudally, areas 35 and 36 are situated inside and dorsal to the fundus of the posterior rhinal sulcus. Agranular insular cortex and granular insular cortex form the cortical areas located rostral to the perirhinal cortex. These regions correspond to AIp and VISC according to Swanson (1998) or AIP, DI, and GI according to Paxinos and Watson (1998). Area 36 is located caudal to AIp and VISC, and area 35 is located caudal to AIp. If one follows the insular cortex adjacent to the rhinal sulcus in a rostrocaudal direction, the underlying claustrum (Fig. 4A–C) gradually becomes smaller until it is no more than a small ball of disorganized, darkly stained, rather large cells located beneath layer VI and underlying the rhinal sulcus. As the ball of claustral cells flattens and disappears, the rhinal sulcus becomes more deeply invaginated (Figs. 4D–I). When the claustral cells are no longer visible, insular cortex is no longer present and is replaced by the perirhinal cortex. The border as identified by the absence of claustral cells below layer VI of the cortex occurs between -2.45 and -2.80 mm relative to bregma (Paxinos and Watson, 1998), in most cases usually falling closer to -2.80 mm. In some

cases, as in the case shown here, area 35 appears at a more rostral level than does area 36.

In lower magnification photomicrographs, insular cortex can be identified by its three-layered look (Fig. 5A). The cellular layers divide into thirds such that the superficial layers (II–IV) and deep layer (VI) appear darker than the intervening layer V, which has cell-sparse gaps on either side and in which cells are more sparsely organized. This trilaminar look is not apparent in the caudally adjacent perirhinal cortex (Fig. 5B), rather, there are no cell-sparse gaps and cells of layer V are more densely packed, especially in area 35. Several cytoarchitectonic details also distinguish the rostrally adjacent insular areas from the perirhinal cortex. In contrast to the agranular area 35, VISC has a layer IV that is composed of small granular cells (Fig. 6A). AIp is better described as dysgranular because small granular cells are intermixed with deep layer III and superficial layer V, rather than forming a discrete layer (Fig. 6B). Unlike perirhinal cortex, in AIp and VISC, layers V and VI are approximately of the same thickness and can be easily separated from each other. Layer V of VISC and AIp is broad and composed of medium to large, darkly stained pyramidal cells and is continuous across the two regions, forming a broad, homogeneous band with cells of similar size, shape, staining characteristics, and packing density (Figs. 5A, 6A,B). When the perirhinal cortex begins, the single homogeneous, band-like layer V that joins VISC and AIp is no longer present (compare Fig. 5A and B). The layer V cells are smaller and more densely packed and one sees the characteristic arcing organization of cells in area 35.

Area 36 cytoarchitecture. Area 36 is bordered dorsally by Te_v , ventrally by area 35 and caudally by the postrhinal cortex (Fig. 7). In general, area 36 is characterized by a patchy layer II composed of aggregates of round or polygonal, lightly-staining, medium-sized cells. In most cases, small dark pyramids are mixed in with the larger round cells, and the smaller pyramids become more numerous as one proceeds caudally. Layer II of Te_v also appears patchy in some animals, especially at rostral levels, but can be distinguished from area 36 because the cells are more typically pyramid-shaped and usually more lightly stained (Fig. 8A). In area 36, granular cells are apparent, but do not form a discrete layer (Fig. 8B–D), rather, layer IV appears to merge with layer V. There is no cell-sparse gap on either side of layer V, as is sometimes observed in the dorsally located Te_v (Fig. 8A). These cell-sparse gaps in Te_v are not observed in all cases, but, when present, they provide a convenient criterion for identifying the area 36d/ Te_v border. Area 36 is also characterized by a thick, bilaminar layer VI that distinguishes it both from the dorsally adjacent Te_v and the ventrally adjacent area 35. The outer sublayer is similar to layer V in packing density and staining characteristics of cells. In the inner sublayer, cells are flattened parallel to the surface of the external capsule. This bilaminar layer VI, as well as the patchy layer II, are probably the features of area 36 that are seen most reliably across individual animals.

Area 36 has three subfields: areas 36d, 36v, and 36p. Areas 36d and 36v lie along side one another in the dorsoventral plane and occupy the rostral two-thirds of the perirhinal cortex (Fig. 2). Area 36p occupies the caudal third. Area 36d is composed of radially oriented cells in layers II–V that differentiate it from area 36v in which the cells of these layers do not have any systematic orienta-

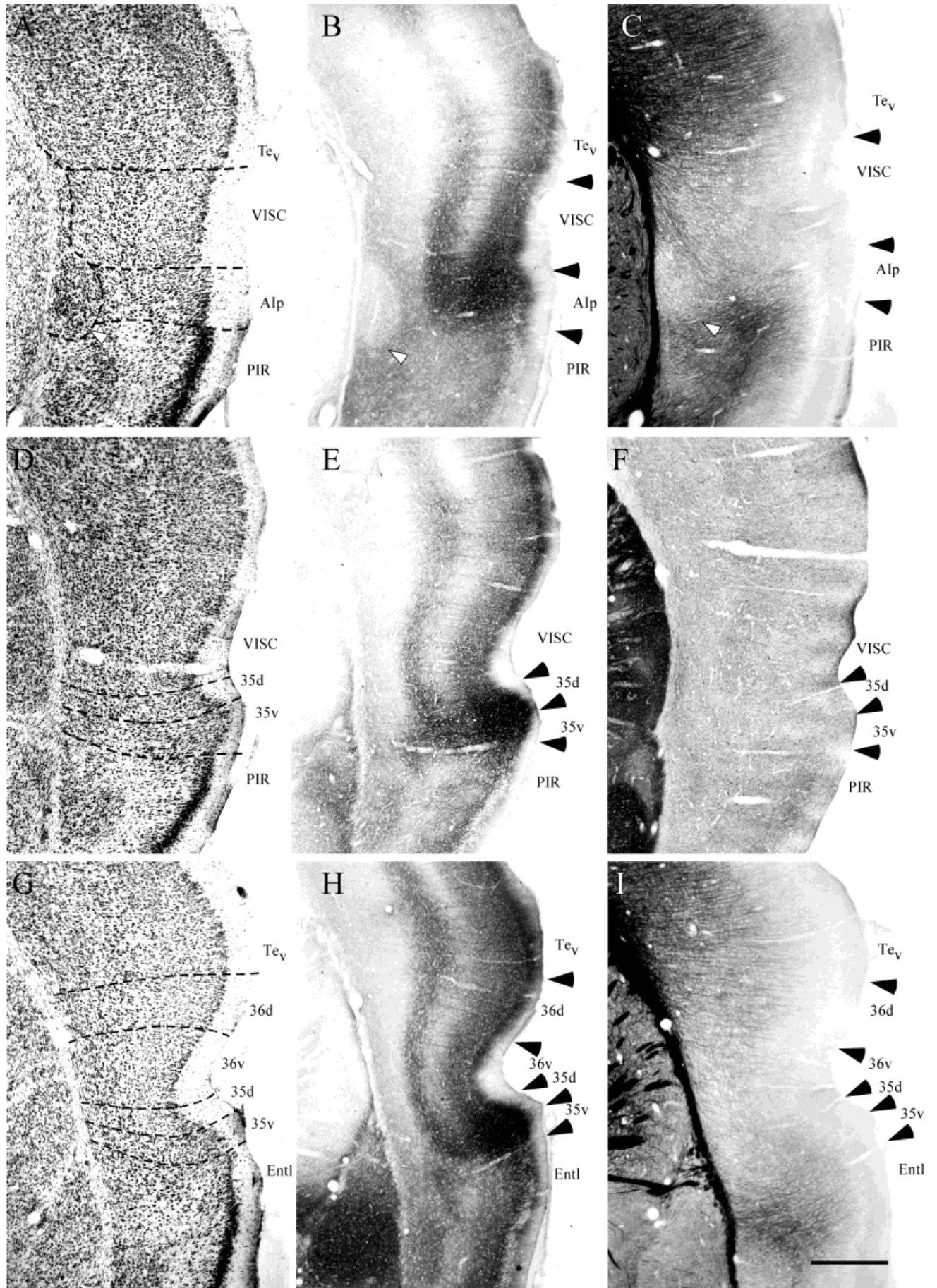


Figure 4

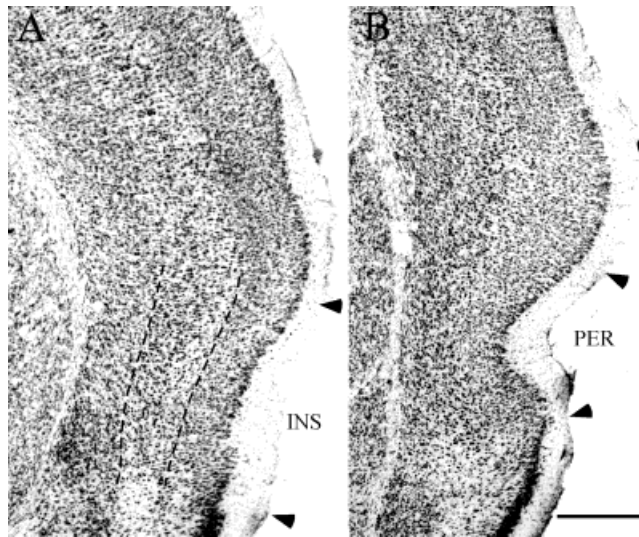


Fig. 5. Low-powered photomicrographs of hemisections at the level of insular cortex at -1.40 mm relative to bregma (A) and perirhinal cortex at -2.80 mm relative to bregma (B) showing a defining feature of insular cortex. AIp and VISC share a homogeneous layer V, which at low power appears more lightly stained than the deeper layer VI or the superficial cellular layers II–III giving the combined VISC/AIp region a trilaminar appearance as described in Krieg's (1946b) description of the posterior insular cortex. This is contrasted with the perirhinal region in which layer V of area 36 differs cytoarchitectural from that of 35, thus not giving the signature trilaminar appearance of the rostrally adjacent region. Scale bar = $500 \mu\text{m}$.

tion (Fig. 8B,C). Compared with the dorsally adjacent cortex, area 36d has a narrower layer VI and a narrower layer V. Deep layer VI contains elongated cells that lie parallel to the external capsule. Small polygonal cells that have a disorganized, clumpy arrangement populate superficial layer VI. Layer V has large, darkly stained pyramidal cells that form a size gradient such that more superficial cells are smaller. The cells in layer III of 36d are similar in shape and size to those in layer II but are less densely packed and do not show the characteristic patchiness of layer II.

In some cases, area 36v appears at a slightly more rostral level than area 36d. The distinguishing characteristic of area 36v is that it does not have the radial appear-

Figure 4. Coronal sections showing insular and perirhinal regions at three rostrocaudal levels. Adjacent sections stained for Nissl material (A), heavy metals using Timm's method (B), and myelin (C) show VISC and AIp at approximately -1.40 mm relative to Bregma (Paxinos and Watson, 1998) corresponding to Figure 3A. Open arrows indicate the location of the claustrum. Adjacent coronal sections stained for Nissl material (D), heavy metals using Timm's method (E), and acetylcholinesterase (F) show the perirhinal area 35 at approximately -2.56 mm relative to Bregma (Paxinos and Watson, 1998) corresponding to Figure 3B. Adjacent coronal sections showing the perirhinal areas 35 and 36 and adjacent cortical regions. Sections stained for Nissl material (G), heavy metals using Timm's method (H), and myelin (I) show perirhinal areas 35 and 36 at approximately -2.80 mm relative to Bregma (Paxinos and Watson, 1998) corresponding to Figure 3C. For this and all subsequent photomicrographs, dashed lines or closed arrows indicate cytoarchitectonic borders. Scale bar = $500 \mu\text{m}$.

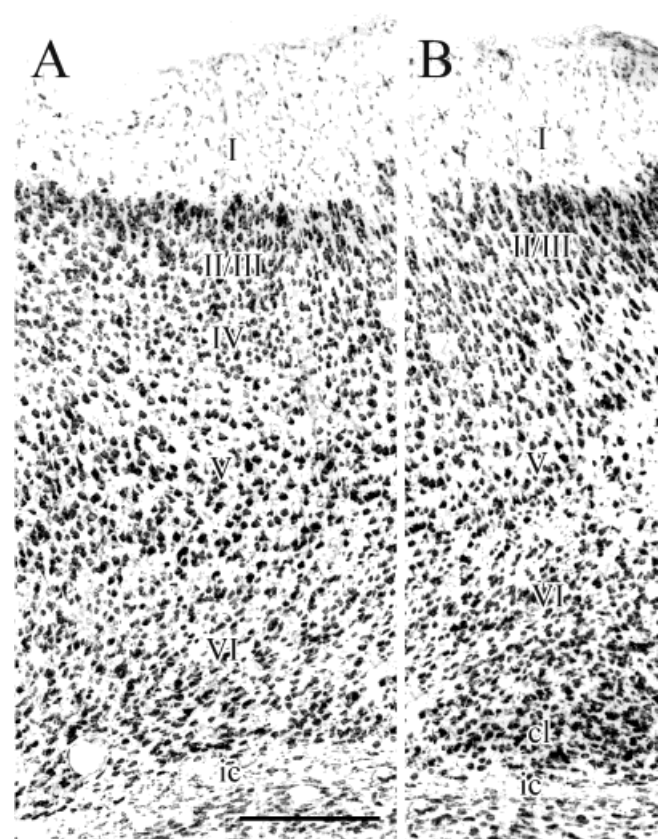


Fig. 6. High-powered photomicrographs of the cortical layers of the insular cortex at -1.40 mm relative to bregma. VISC has a discrete layer IV (A), whereas layer IV of AIp is more accurately described as dysgranular (B). Layer V of VISC and AIp exhibits cells of similar size, staining characteristics, and packing density. Scale bar = $250 \mu\text{m}$.

ance exhibited by area 36d (Figs. 7A, 8B,C). As in area 36d, layer VI of 36v is composed of superficial and deep portions, but overall the layer is narrower than in 36d. The deep layer VI cells are elongated but are not quite as long or flat as those seen in area 36d. Layer V is composed of medium-sized, darkly stained pyramidal cells that do not have any particular orientation. Proceeding caudally, the cells become progressively smaller, darker, and more angular. The superficial cellular layers also lack the radial organization seen in the dorsally adjacent area 36d. Layer III is composed of medium-sized round or polygonal cells that are homogeneously distributed throughout the layer. As with area 36d, the cells in layer III are similar in shape and size to those in layer II but are less densely packed. Layer II exhibits the patchiness that is characteristic of area 36 (Fig. 8C).

The rostral border of area 36p is located at the rostrocaudal level at which the lamina dissecans (cell-sparse layer IV) of dorsolateral entorhinal cortex is observed to extend dorsomedially beneath the perirhinal cortex (Fig. 7G–I). Usually at this level, the caudal limit of the granule cell layer of the dentate gyrus disappears from cortical sections. There are several structural characteristics that distinguish area 36p from the rostrally adjacent subdivisions. First, although area 36p is still laminated, there are

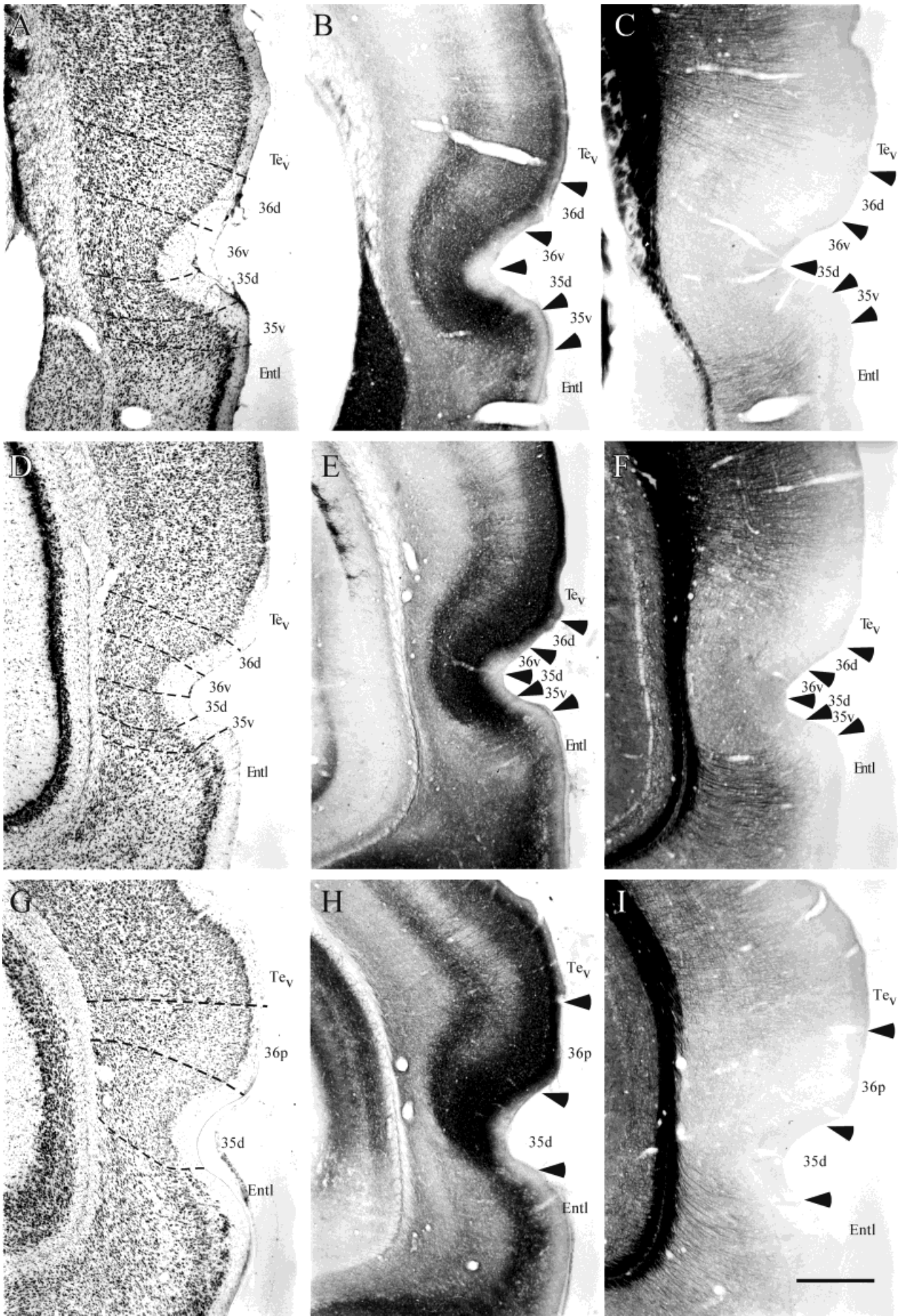


Figure 7

medium-sized, darkly stained, roundish cells mixed in with deep layer V and superficial layer VI, so that, overall, a more homogeneous packing density yields a less laminar appearance of the region (Fig. 8D). Moreover, area 36p has a layer VI that is not as clearly bilaminated as in area 36d. The second feature is that the cells in area 36p are less radially oriented than those seen in area 36d. Area 36p is best distinguished from the dorsally adjacent Te_v by differences in layer II. At this level, layer II of Te_v has a thin or compressed outer layer that differs markedly from the patchiness observed in area 36. Additionally, the cells of layer V of Te_v are larger than in 36p.

Area 36 histochemistry. In general, the perirhinal cortex is distinguished from the dorsally adjacent and ventrally adjacent cortical regions by the absence of heavy myelination (Figs. 4I, 7C,F,I). There are, however, a few subtle regional and subregional differences. In area 36d myelinated fibers are more obvious in deep layers and are progressively less prominent as one follows them from white matter to the superficial layers. The fibers usually end in mid-layer V. Myelinated fibers are also less and less prominent as one follows layer V ventrally from the dorsal border of area 36d. Thus, area 36d contains more myelinated fibers in deep layers than area 36v, and area 36v contains more than area 35. In overstained material (not shown), it is possible to see thin, lightly stained, myelinated fibers in layer I of the perirhinal cortex. These fibers are confined to an inner sublayer that varies in thickness from region to region. The thickness of the outer, nonmyelinated margin distinguishes area 36 from the ventrally adjacent area 35 and from the dorsally adjacent area Te_v ; the myelin-free margin is thicker in area 35 (two-thirds of the layer) than area 36 (one-half), and thicker in area 36 than in Te_v (one-fourth of layer I).

In material stained for heavy metals by Timm's method, area 36 cortex exhibits a laminar pattern of label that is similar in some ways to Timm's staining observed in sensory cortical regions, i.e., deep layer I and layer II stain very darkly, layer III is moderately dark, layer IV is light, and staining in layer V exhibits sublayers. Area 36d is distinguishable from Te_v by the pattern of staining in layer V (Figs. 4H, 7B,E,H). In both regions the staining exhibits a trilaminar pattern, with the middle half of layer V staining more darkly than superficial or deep quarters of layer V. In Te_v however, each sublayer is broader than in area 36, especially the deep sublayer. Moreover, the dark band in middle layer V is lighter in Te_v than in area 36d. Similarities as well as differences be-

tween areas 36d and 36v are apparent; in both subdivisions deep layer I stains darkly, but superficial layer I does not. In area 36d, however, the darkly stained portion of layer I is both darker and broader than in 36v. There are also differences in layer V staining in that the superficial, light sublayer observed in Te_v and area 36d disappears in area 36v. The Timm's staining pattern in area 36p is more similar to that of area 36d than to area 36v or area 35 in that the light sublayer in superficial layer V is present (Fig. 7H).

Area 35 cytoarchitecture. Area 35 is bordered dorsally primarily by area 36 and ventrally and caudally by the entorhinal cortex. Just as area 36v may appear at a more rostral level than area 36d, area 35 may appear at a more rostral level than area 36 (Figs. 3B, 4D–F). Area 35 is distinguished from the dorsally adjacent area 36 by several characteristics. First, layer I tends to be thicker, although this does not change sharply at the border between the two regions. The thickness of layer I in mid-dorsoventral area 36 is approximately 50% of that in mid-dorsoventral area 35 (e.g., Figs. 4G, 7G). It may be, however, that the thickened layer I is a feature that is more appropriately associated with the rhinal sulcus than with a cytoarchitectural region. Second, the cells in area 35 exhibit a modified radial organization such that they form a shallow U-shaped arc beginning at the pial surface ventral to the rhinal sulcus and ending at the white matter deep to the rhinal sulcus (e.g., Fig. 7A,D). Third, area 35 is characterized by large, darkly stained, heart-shaped pyramidal cells in layer V. These cells are progressively smaller proceeding caudally (Fig. 8E). Although similar cells are seen in layer V of area 36v, there are fewer and they are not as distinctively heart shaped or as large. Heart-shaped cells become progressively smaller as one moves caudally (Fig. 8F). Another difference is that layers II and III of area 36 are more clearly separated into two distinct layers as compared with area 35.

Area 35 comprises two subfields, areas 35v and 35d. Area 35v sometimes appears slightly more rostrally than area 35d, but area 35d usually extends farther caudally (Fig. 7G–I). Area 35v is distinguished from area 35d in three ways (Fig. 8E,F). First, the arcing organization of cells across all layers is especially prominent in 35v, where the cells form an arc that bends dorsally so that layer VI of area 35v merges with the layer VI of 35d. Second, in 35d the layer II/III cells form clumps, whereas the cells in layer II/III of area 35v are slightly elongated perpendicular to the pial surface, giving them a "streaming" appearance. Third, in 35d the neuronal density is lower in the deep portion of layer II/III, which gives the appearance of a cell-sparse gap between layers III and V. This feature tends to be more evident at caudal levels (Fig. 8B).

Area 35 histochemistry. Staining for heavy metals (Figs. 4E,H, 7B,E,H) and for myelin (Figs 4I, 7C,F,I) provides useful markers for the ventral border of area 35. In contrast, acetylcholinesterase staining, although useful for identifying subcortical landmarks, shows only subtle differences between cortical regions and is not particularly useful in identifying the cortical boundaries in question (Fig. 4F).

As shown in Figure 7C, the ventrally adjacent entorhinal cortex exhibits a dense plexus of myelinated fibers, which are virtually nonexistent in area 35. Area 35 has few myelinated fibers when stained with a standard pro-

Fig. 7. Coronal sections showing the perirhinal areas 35 and 36 and adjacent cortical regions at three rostrocaudal levels. Adjacent sections stained for Nissl material (A), heavy metals using Timm's method (B), and myelin (C) show perirhinal regions at approximately -3.80 mm relative to Bregma (Paxinos and Watson, 1998) corresponding to Figure 3D. Open arrows indicate the location of the claustrum. Adjacent coronal sections stained for Nissl material (D), heavy metals using Timm's method (E), and myelin (F) show the perirhinal regions at approximately -5.30 mm relative to Bregma (Paxinos and Watson, 1998) corresponding to Figure 3E. Adjacent coronal sections show perirhinal areas 35 and 36 and adjacent cortical regions. Sections stained for Nissl material (G), heavy metals using Timm's method (H), and myelin (I) show perirhinal areas 35 and 36 at approximately -6.72 mm relative to Bregma (Paxinos and Watson, 1998) corresponding to Figure 3F. Scale bar = 500 μ m.

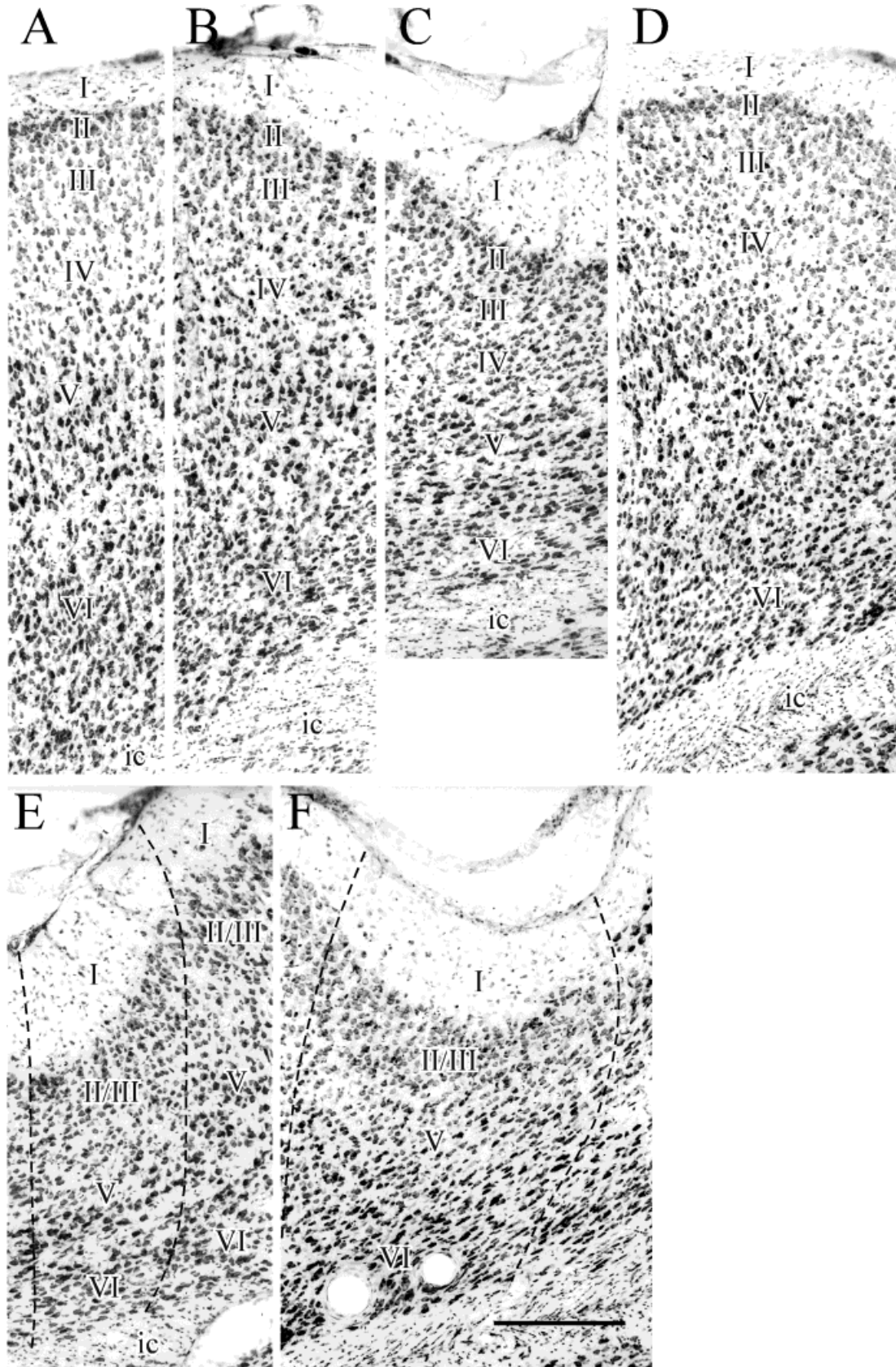


Fig. 8. High-powered photomicrographs of the cortical layers of areas Te_v (A), 36d (B), 36v (C), 36p (D), 35d (E), and 35v (F). A-C and E correspond to -3.80 relative to Bregma, and D and F correspond to -6.72 mm relative to Bregma. Scale bar = $250 \mu\text{m}$.

tolcol and observed at low magnification. In overstained material (not shown), it is possible at high magnification to see thin, lightly stained myelinated fibers in layer I of area 35. The thickness of the outer, nonmyelinated margin distinguishes area 35 from the dorsally adjacent area 35 in that the myelin-free margin is thicker in area 35 (two-thirds of the layer) than area 36 (one-half). Myelin stain does not distinguish between area 35 subregions.

With Timm's staining, area 35 layers II–V stain darkly for heavy metals, in contrast to the ventrally adjacent entorhinal cortex, which exhibits heavy staining only in layer II and only in a mottled pattern. Timm's stain also provides useful criteria for the dorsal border of the region. In the dorsally adjacent cortex, in layer V of area 36, only the middle portion of the layer is darkly stained, revealing a trilaminar appearance, whereas in area 35 layer V is completely filled in such that the layer has a homogenous, dark appearance.

Postrhinal cortex

The postrhinal cortex is located caudal to area 36p and largely dorsal to the rhinal sulcus (Figs. 2, 3). In most cases, the postrhinal cortex arises at the caudal limit of the angular bundle when subicular cells are no longer present in coronal sections. Another landmark is the shortening of the presubiculum in the dorsoventral dimension and the imposition of a cell-sparse region deep to presubiculum that borders the underlying white matter. Like the perirhinal cortex, the postrhinal cortex is associated with the rhinal sulcus. Rostrally, the superficial layers lie in the fundus of the rhinal sulcus, but the deep cortical layers underlying the fundus belong with the ventrally adjacent entorhinal cortex (Fig. 9A–C). Caudally the region assumes a position above the fundus (Fig. 9D–H). If one imagines a caudal extension of the rhinal sulcus it would rise at caudal levels and wrap around the caudal pole of the brain just ventral to the postrhinal cortex. If the cortex surrounding the rhinal sulcus and its imagined caudal extension could be straightened and flattened, the postrhinal cortex would form a long narrow strip largely dorsal to the sulcus and similar to the shape of the perirhinal cortex, but shorter along the longitudinal axis (Fig. 2C). The postrhinal cortex rises steeply and wraps obliquely around the caudal pole of the brain. Thus, its conformation is difficult to discern in the coronal plane. Because of the oblique cut in the coronal sections, the region extends farther dorsally and is limited in its rostrocaudal extent. Even unfolded maps can be misleading because of the tendency of surface areas of polar regions to be underrepresented. In sagittal sections, its long, narrow shape is more easily identified.

The dorsal border of the postrhinal cortex is difficult to discern but is reliably identified relative to certain structural landmarks, particularly the location of the parasubiculum. The parasubiculum is on the medial cortical surface and is easily identified in cell-stained and acetylcholinesterase-stained sections. The dorsal border of POR on the lateral cortical surface is located directly across from the mid-dorsoventral level of the parasubiculum (Fig. 3G,H). Caudally, the parasubiculum also is useful in identifying the ventral border of the postrhinal cortex. At its caudal limit, the parasubiculum extends laterally more than halfway across the cortex and lying between the postrhinal cortex and entorhinal cortex (Figs. 3I, 9G,H). Thus, at this level, the postrhinal cortex has a

modified triangular shape such that PaSub (medially) and the entorhinal cortex (laterally) form one side of the triangle and the pial surface and VIS1 form the other two sides.

Postrhinal cytoarchitecture. Perhaps the most characteristic cytoarchitectonic feature of the postrhinal cortex is its homogeneous packing density across layers II–IV and the resulting lack of a prominent laminar structure (Fig. 9D). It is difficult to differentiate deep from superficial layers because the layers appear to blend into one another. A second characteristic of the region as visualized in the coronal plane is that all layers become unusually broad as one moves from superficial to deep (Fig. 10). This thickening, however, is entirely a function of the conformation of the region and the plane of section; postrhinal cortex wraps around the caudal pole of the brain and, at these levels, the coronal plane cuts obliquely across the radial axis of the cortex. A third characteristic of the postrhinal cortex is also due to conformation: the surface of the ventral portion of the region that is located dorsal to the rhinal sulcus is tightly convex such that deeper layers are compressed. Similar to cortical layers of gyri of the primate brain, the length of the superficial layers is longer than the length of the deeper layers. As a result, only a very narrow segment of layer VI is associated with the superficial layers of ventral postrhinal cortex (Fig. 9A–C). Although the lack of a prominent laminar structure is accentuated in coronal sections, this feature is also apparent in sagittal sections (not shown). The broadening of deeper layers, however, is not apparent in sagittal sections in which layers I–III, V, and VI occupy approximately one-third each of the radial extent of the cortex.

The postrhinal cortex has two subfields: PORv and PORd. PORv is located dorsal to the entorhinal cortex and caudal to area 36p. In the coronal plane, in rare cases, PORv emerges rostral to PORd, and in these cases, PORv is located ventral to 36p at its most caudal levels. In most cases, however, area 35d occupies this position (Fig. 3F).

PORd is located dorsal to PORv but sometimes begins slightly more caudally than PORv. Cells in PORd layer III (Fig. 10A) are more heterogeneous in size, shape, and color and are more organized and radial in appearance than in the ventrally adjacent PORv (Fig. 10B). Layers II and III are each composed of a homogeneous population of medium-sized, lightly stained round and polygonal cells, but the cells are more densely packed in layer II. In some cases, small dark pyramids are mixed into layer II. In the dorsally adjacent Te_v , packing density is also higher in layer II; however, layer II and III cells of the dorsally adjacent Te_v at this level are small, round, and darkly stained and do not have a radial appearance as in PORd (Fig. 9A). A granular layer is distinguishable, but less so at caudal levels. Layer V of PORd is slightly narrower than in PORv. Layer V differs from the dorsally located Te_v in that Te_v layer V is more open and sparsely populated, and the cells are larger.

There are several typical cytoarchitectonic features of PORv. Perhaps the most distinctive is the presence of ectopic layer II cells at rostral levels of the region near the border with entorhinal cortex (Fig. 10B). These ectopic cells are present in all cases, but they vary in prominence. Layer II cells are moderately large, light, and round, but not as large as those seen in perirhinal cortex. Rostrally, layers II and III can be distinguished from one another because layer III cells are less organized and less densely

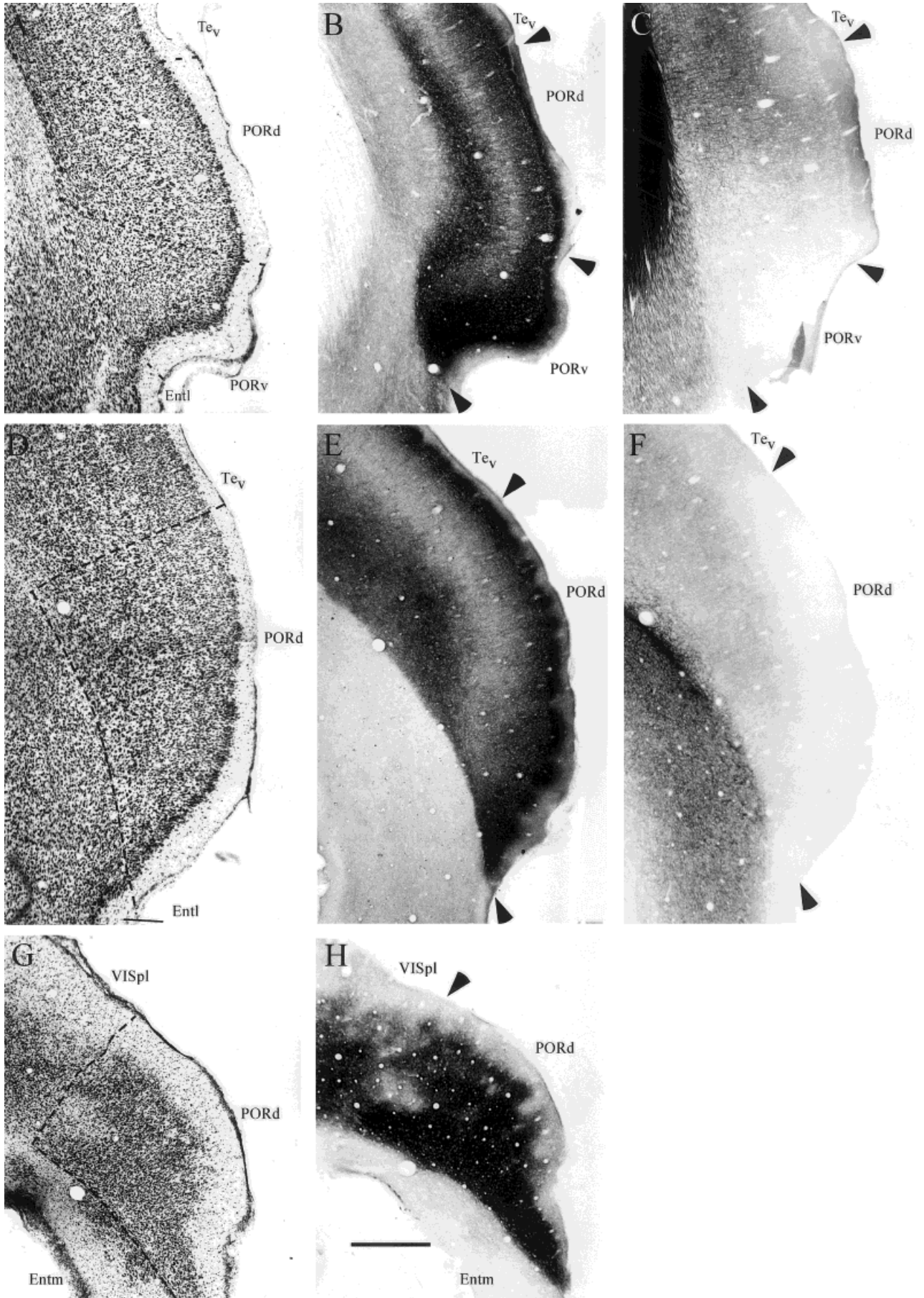


Figure 9

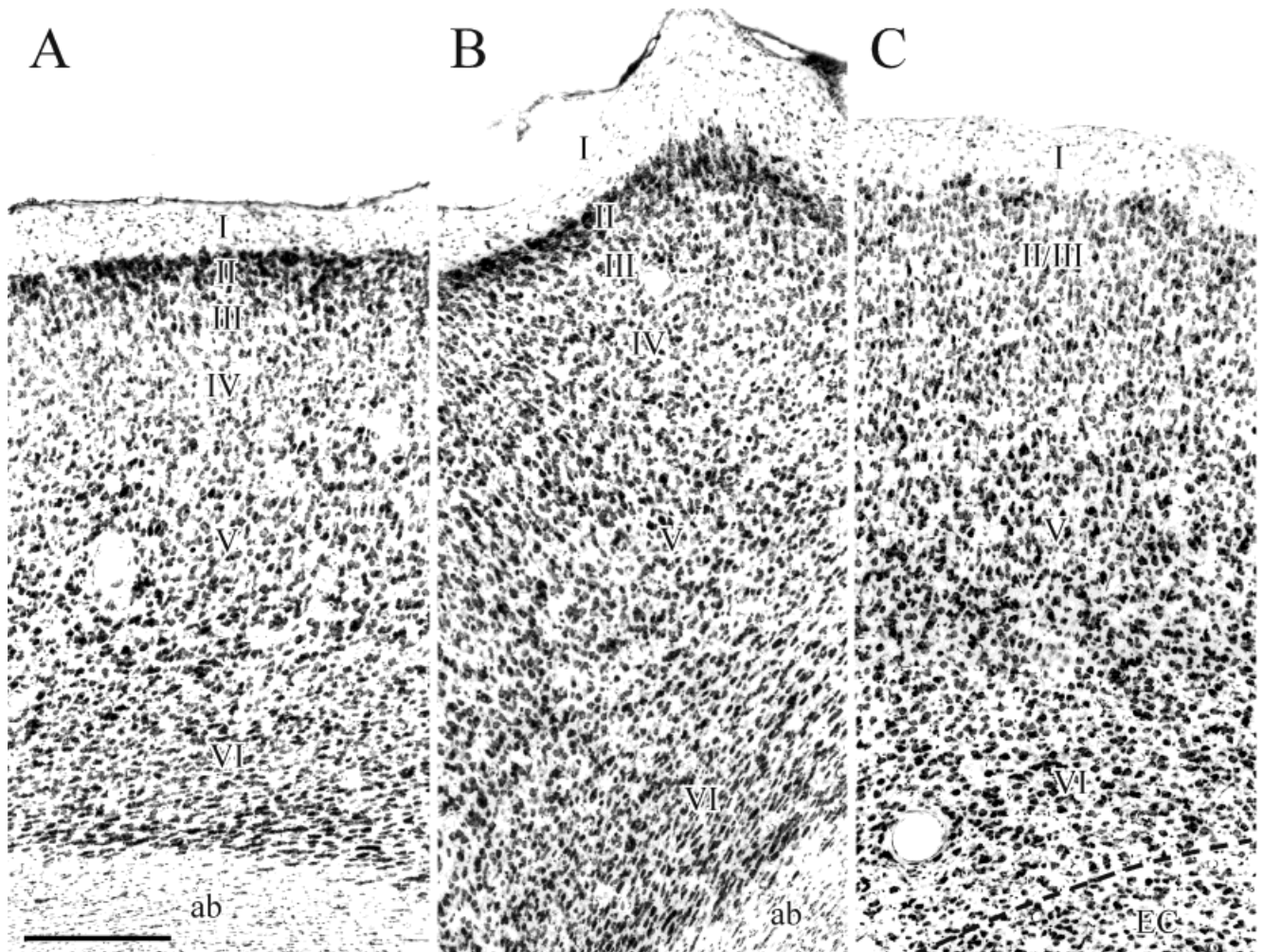


Fig. 10. High-powered photomicrographs of the cortical layers of areas PORd (A) and PORv (B) at -7.64 mm relative to Bregma. A more caudal view of PORd (C) corresponds to -8.30 mm relative to Bregma. Scale bar = $250 \mu\text{m}$.

packed. Caudally, however, layer II is not easily distinguished from Layer III (Fig. 10C). PORv is dysgranular at all rostrocaudal levels, such that granule cells fill in between layers III and V, giving an overall homogeneous appearance to the region. Rostrally, the width of layer V appears broader than in the dorsally located PORd, but this may be secondary to the curvature of the cortex at this

level. Layer V is composed of small pyramid-shaped cells. Layer VI, which is fused together with layer V, is composed of fusiform cells and elongated pyramids that are oriented almost parallel with the angular bundle; however, only a small portion of layer VI is associated with PORv.

Postrhinal histochemistry. Other markers distinguish subregional boundaries and outer borders of the postrhinal cortex. Timm's stain (Fig. 9B,E,H) reveals a laminar pattern in the PORd of postrhinal cortex such that the inner, but not outer, sublayer of layer I stains darkly, layers II and III stain moderately, and layer IV is lightly stained. Layer V exhibits a trilaminar pattern such that the middle portion is darker than the superficial and deep sublayers stain only lightly. Unlike PORd, PORv does not show a strong laminar pattern with Timm's stain. The outer layer I, deep layer V, and layer VI stain lightly, but all layers in between are darkly stained. Timm's stained material clearly distinguishes the ventral borders with the parasubiculum and entorhinal cortex, which do not stain positively for heavy metals. In the dorsally adjacent Te_v , bands distinguished by staining for heavy met-

Figure 9 Coronal sections showing the postrhinal cortex and adjacent cortical regions at three rostrocaudal levels. Adjacent sections stained for Nissl material (A), heavy metals using Timm's method (B), and myelin (C) show postrhinal cortex at approximately -7.64 mm relative to Bregma (Paxinos and Watson, 1998) corresponding to Figure 3G. Adjacent coronal sections stained for Nissl material (D), heavy metals using Timm's method (E), and myelin (F) show the postrhinal cortex at approximately -8.30 mm relative to Bregma (Paxinos and Watson, 1998) corresponding to Figure 3H. Adjacent coronal sections showing the perirhinal areas 35 and 36 and adjacent cortical regions. Sections stained for Nissl material (G) and heavy metals using Timm's method (H) show postrhinal cortex at approximately -9.16 mm relative to Bregma (Paxinos and Watson, 1998) corresponding to Figure 3I. Scale bar = $500 \mu\text{m}$.

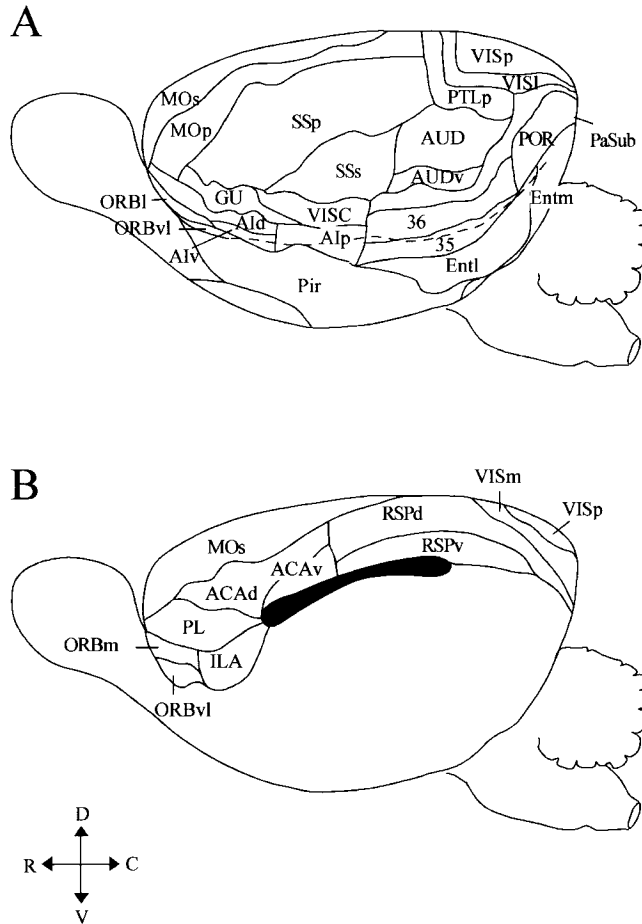


Fig. 11. Lateral (A) and medial (B) surface views of the rat brain. The schematic demonstrates the location of the perirhinal cortex (areas 35 and 36) and the postrhinal cortex. Also shown are the cortical regions defined by Swanson (1992) that were used to analyze retrogradely labeled cells resulting from perirhinal and postrhinal injection sites in a prior paper (figure adapted from Burwell and Amaral, 1998). Those data were used here to conduct confirmatory analyses of the regional definitions of perirhinal areas 35 and 36 and the postrhinal cortex.

als exhibit subtle differences compared with the postrhinal cortex. In particular, the dark inner sublayer of V is narrower. Also, layer I is more equally divided into an inner darkly stained layer and an outer lightly stained layer.

Myelin-stained material (Fig. 9C,F) yields a profile for the postrhinal cortex similar to that of the perirhinal cortex, i.e., few fibers stain for myelin, especially ventrally. Although the density of myelinated fibers increases as one follows the region dorsally, the staining is much more prominent in Te_v , where layers VI and V exhibit a dense plexus of myelinated fibers.

In acetylcholinesterase preparations, stained fibers in the postrhinal cortex are visible in all layers. Parasubiculum, however, stains more darkly, clearly marking the ventromedial border with the entorhinal cortex. The ventrolateral border is also well marked in this material in that fibers in layer II of the entorhinal cortex stain more robustly for acetylcholinesterase than fibers located in the dorsally adjacent postrhinal cortex.

TABLE 1. Cluster Solutions¹

| Case | Injection site location | Cluster solution |
|-------|-------------------------|------------------|
| 102DY | Area 35 | 1 |
| 132FB | Area 35 | 1 |
| 112DY | Area 35 | 1 |
| 108FG | Area 35 | 1 |
| 100DY | Area 35 | 1 |
| 097DY | Area 36 | 2 |
| 099DY | Area 36 | 2 |
| 116DY | Area 36 | 2 |
| 120FB | Area 36 | 3 |
| 098DY | Area 36 | 3 |
| 132DY | Area 36 | 3 |
| 094FB | Area 36 | 3 |
| 120DY | Area 36 | 3 |
| 097FB | POR | 4 |
| 102FB | POR | 4 |
| 098FB | POR | 4 |
| 100FB | POR | 4 |
| 095DY | POR | 4 |
| 099FB | POR | 4 |

¹The cluster solution was robust with respect to methods of clustering in that similar groupings were obtained by two other commonly used clustering algorithms, the Average Linkage method and the Centroid method. Note that the injection sites in ventral and dorsal area 36 clustered together, clusters 2 and 3, respectively.

Confirmatory connective analyses

As detailed in Materials and Methods, the availability of extensive and empirical cortical afferent data for the perirhinal and postrhinal cortices from a prior study (Burwell and Amaral, 1998a) permitted empirical analyses of the regional definitions for perirhinal areas 35 and 36 and the postrhinal cortex. Cluster analysis was employed to examine how retrograde tracer injections placed in the perirhinal and postrhinal cortices would be grouped based solely on the pattern of retrogradely labeled cells in the neocortical regions shown in the surface views in Figure 11 (Burwell and Amaral, 1998a). Table 1 lists the retrograde tracer cases analyzed and the location of the injection sites. The cluster analysis, which included 19 injection sites located in the three target areas, addressed the issue of whether areas 35, 36, and the postrhinal cortex could be distinguished on the basis of cortical afferentation. There was a marked flattening of the SPRSQ curve at the 4-cluster solution, indicating that the variance explained by four groups would not be substantially improved by the addition of more groups. Figure 12A shows the location of each of the 19 injection sites color-coded for cluster membership. Three injection sites were misclassified according to neuroanatomical location, i.e., areas 35 and 36 or the postrhinal cortex. Sites 116DY, 097DY, and 099DY were clustered together, but were not classified as belonging to the cluster that included the remaining five injections area 36 (Fig. 12A). Notably, each of these sites was located in ventral area 36. Classification according to the cluster solution was statistically highly similar to the classification according to neuroanatomical location of the injection sites ($R = 0.87$).

To determine how neocortical input contributed to the grouping of injection sites, the regional patterns of retrogradely labeled cortical cells that differentiated clusters were analyzed by multivariate analysis of variance (MANOVA) followed by pairwise comparisons. Following MANOVA on the full complement of cortical input region variables (significant Region \times Cluster interaction, $P < 0.0001$), separate pairwise analyses of Cluster were completed for each cortical regional variable used in the cluster analysis. The results of all pairwise comparisons are

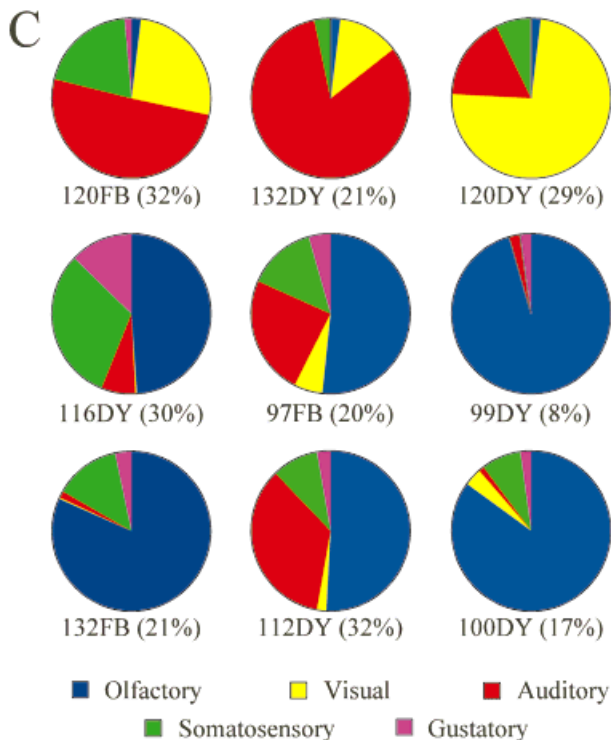
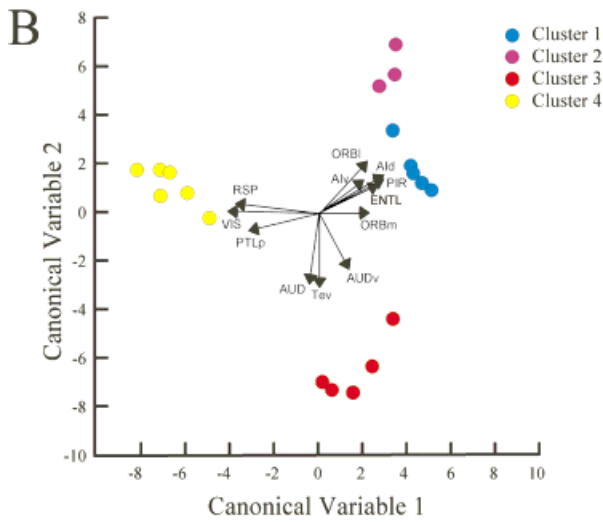
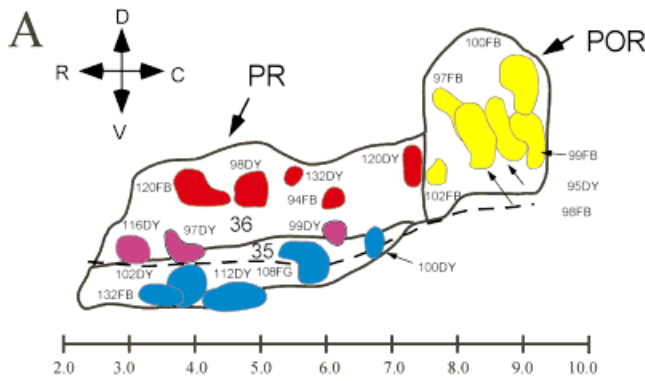


TABLE 2. Variables Significantly Different Across Clusters¹

| Cluster | Cluster | | |
|---------|--|--|---|
| | 2 | 3 | 4 |
| 1 | AUDv Te _v RSPd RSPv PTLp VISl VISm VISp | ORBI ORBm Alv PIR PTLp RSPd RSPv VISl VISm VISp | PL AId PIR PTLp RSPd RSPv VISl VISm VISp Entl |
| 2 | | ORBI AUD Te _v | AId PIR AUD Te _v Entl |
| 3 | | | PIR Entl |

¹Variables correspond to numbers of retrogradely labeled cells in the cortical regions shown in Figure 11. Listed are all variables that were significantly different on pairwise comparisons among clusters with a significance level of $P < 0.005$. Cluster classification corresponds to neuroanatomical classification as follows: area 35 (1), area 36 (2 and 3), and the postrhinal cortex (4).

shown in Table 2, which includes each variable that distinguished two clusters at a significance level of $P < 0.005$. Membership in the four clusters conformed largely to regional boundaries, i.e., area 35 (cluster 1), area 36 (clusters 2 and 3), and postrhinal cortex (cluster 4).

To illustrate the relationship of significant regional cortical input variables to cluster organization, the results of a canonical discriminant analysis of the cluster solution are shown in Figure 12B. Only those variables that were significant on pairwise comparisons were entered into the analysis. Regional variables that exhibited similar patterns of results on the pairwise comparisons were combined across subregions to further reduce the numbers of variables, e.g., RSPd and RSPv were combined to form RSP. The biplot in Figure 12B shows the plane described by the first two canonical variables identified by the discriminant analysis. These canonical variables are linear combinations of the cortical input variables and accounted for 80% of the total between cluster variance. Each of the cortical input variables is plotted as a vector from the origin to the point described by its canonical coefficients. The vectors show visually what is apparent from the cluster and multivariate analyses, i.e., the patterns of retro-

Fig. 12. Results of cluster and discriminant function analyses of retrograde tract tracer injections in the perirhinal and postrhinal cortices (Table 1) based on regional patterns of retrogradely labeled cells in neocortex. **A:** Cluster solution. An unfolded map of the perirhinal and postrhinal cortices showing the location of injection sites included in the analysis. Cluster membership is color coded. **B:** A canonical discriminant analysis of the cluster solution. Each retrograde experimental case is identified by its membership in a cluster and placed on the graph according to its score on the first two canonical variables. Additionally, the cortical input variables that significantly distinguished clusters 1–4 from each other (Table 2) are plotted as vectors from the origin. Because the direction and relative lengths of the vectors are important, the vector lengths were multiplied by a constant ($4\times$) to make them more visible. **C:** Proportions of labeled cells in unimodal regions are shown for nine injection sites distributed in the perirhinal cortex. The proportion of total cortical input accounted for by unimodal input is shown in parentheses. Thus, cells labeled in unimodal associational regions accounted for 8–32% of total labeled cortical cells for each injection site.

gradely labeled cells in visuospatial, orbitofrontal, temporal, and insular regions account for much of the variance across clusters. The implication is that differences in input from these regions differentiate area 35, area 36, and the postrhinal cortex from one another.

These confirmatory analyses provide evidence that perirhinal areas 35 and 36 and the postrhinal cortex in the rat, as identified by cytoarchitectural and histochemical criteria, are also anatomically distinct in connectional organization.

DISCUSSION

The present study provides the first detailed description of the cytoarchitecture and myeloarchitecture of the rat perirhinal and postrhinal cortices. Histochemical data are also presented. The structural analysis suggested that some borders differ from those used in earlier studies by Burwell and Amaral (1998a,b). Specifically, the rostral border of the perirhinal cortex with insular regions, i.e., the level of the caudal limit of the claustrum in most animals, is slightly more posterior relative to bregma than previously described. An additional difference from the earlier preliminary borders is that area 35 extends farther caudally than was previously appreciated. Each of these borders was adjusted based on descriptive analyses, but they are consistent with connectional findings discussed below.

To summarize the general findings, the perirhinal cortex is dysgranular (area 36) or agranular (area 35) cortex characterized by large heart-shaped cells in layer V, especially in deep layer V. This feature is more prominent in areas 36v and 35 than in area 36d. Layer V cells form a size gradient such that cells are smaller superficially than at deeper levels. The organization of layer V cells tends to be radial in area 36 but not in area 35. Layer VI is bilaminar in both subregions. A prominent feature of area 36 is its patchy layer II. A prominent characteristic of area 35, particularly 35v, is the organization of cells across layers in an arcing formation.

The transition from insular cortex to the perirhinal cortex is most easily seen at low magnification, at which the ball of claustral cells and the trilaminar look of insular cortex is most easily discerned. Moving caudally, when claustral cells are no longer seen and the homogeneous look to layer V of the insular regions disappears, the perirhinal cortex becomes visible. The cortex situated dorsal to area 36 can be distinguished by a more well-defined layer IV, a thinner layer II, and a broader, more sparsely populated layer V. The entorhinal cortex is most easily distinguished from area 35 by the appearance of a lamina dissecans and differences in the size and shape of layer II cells.

At the border between the perirhinal and postrhinal cortices, the most salient feature is the presence of ectopic layer II cells in the rostral and ventral postrhinal region. In coronal sections cut perpendicular to the flat skull stereotaxic position, this feature generally appears at the level of the caudal limit of the angular bundle. The postrhinal cortex is further characterized by a lack of prominent laminar features. The cortex dorsally adjacent to the postrhinal cortex, Te_v , exhibits a more laminar appearance. For example, layers II and III are more easily distinguished from each other and there is a more prominent layer IV. At rostral levels, the postrhinal cortex is distin-

guished from the medially adjacent entorhinal cortex by the absence of the lamina dissecans. At all levels, POR and the entorhinal cortex can be distinguished by differences in staining density using a number of histochemical preparations including Timm's, myelin, parvalbumin, and acetylcholinesterase (this study; Burwell et al., 1995; Dolorfo and Amaral, 1998; Witter et al., 2000)

Nomenclature

Brodman (1909) described three distinct regions associated with the rhinal sulcus in the human brain, area 28 (*area entorhinalis*), area 35 (*area perirhinalis*), and area 36 (*area ectorhinalis*). Regarding the two latter-named regions, in the rodent brain, Brodman was followed by Rose (1929) in the designation of an *area ectorhinalis* and *area perirhinalis* in the mouse brain (Fig. 1A) and by Krieg (1946b) in the designation of areas 35 and 36 in the rat brain (Fig. 1B). Modern descriptions for the rat have sometimes designated the two areas as *area ectorhinalis* and *area perirhinalis* (e.g., Paxinos and Watson, 1998; Swanson, 1998) (Fig. 1C) and sometimes as area 35 and area 36 (Burwell et al., 1995; Naber et al., 1999; Burwell, 2000; Pitkanen et al., 2000). Although the term "perirhinal" has been applied by some to denote only area 35 (e.g., Kosel, 1981; Van Hoesen, 1995), other investigators have used the term perirhinal cortex to denote the combined areas 35 and 36 (e.g., Witter and Groenewegen, 1984; Burwell et al., 1995; Suzuki, 1996; Pitkanen et al., 2000). Insausti et al. (1987) employed connectional criteria to distinguish the monkey perirhinal cortex from the laterally adjacent inferotemporal cortex such that the cortical areas projecting strongly to the entorhinal cortex were considered to belong to the perirhinal region. Because both areas 35 and 36 met this connectional criterion, the term perirhinal was used to denote the combined areas 35 and 36. Burwell et al. (1995) applied similar criteria in the rat. The same terminology was applied even earlier in the cat (Krettek and Price, 1977b; Witter and Groenewegen, 1984). Krettek and Price (1977b) also suggested that the perirhinal cortex in the rat consists of area 35 "perirhinal proper" as well as the dorsally adjacent area analogous to area 36. Thus, the use of the term perirhinal to denote the combined areas 35 and 36 has historical precedence.

Until recently, little was known about the anatomy and function of area 36 in the rat, but it now seems likely, based on corticocortical connectivity and structural characteristics, that area 36 (*area ectorhinalis*) and area 35 (*area perirhinalis*) in the rat are homologous to areas 36 and 35 in the primate (Suzuki and Amaral, 1994a,b; Burwell and Amaral, 1998a,b). These assertions are based on structural similarities as well as cortical and subcortical connectional similarities. Thus, to minimize the use of overlapping terms, to facilitate cross-species comparisons, and to be consistent with prior studies, the author uses the terms area 35 and area 36 for regional neuroanatomical descriptions. The term perirhinal cortex is understood to denote the combined areas 35 and 36. This nomenclature is based on patterns of input to the entorhinal cortex (Burwell and Amaral, 1998b) and the polymodal nature of both divisions (Burwell and Amaral, 1998a). It should be noted, however, that some disagreement still exists as to whether it is appropriate to call area 36 part of the perirhinal cortex.

The term postrhinal cortex was adopted by Burwell and colleagues following the use of the term by Deacon et al.

(1983). Separating the postrhinal cortex from the perirhinal cortex was originally justified based on connectional and cytoarchitectonic differences between the anterior perirhinal cortex and the newly defined postrhinal cortex (Burwell et al., 1995). Subsequent anatomical studies provided additional support for the division (this study, Burwell and Amaral, 1998b; Naber, 1999; Pitkanen et al., 2000). Connectional studies verified that the postrhinal cortex exhibits substantial connectional homology with the parahippocampal cortex in the monkey (Suzuki and Amaral, 1994a,b; Burwell and Amaral, 1998a,b). However, the term parahippocampal cortex was not applied to this region in the rat because cytoarchitectonic criteria supporting such a designation were lacking. Nevertheless, functional homology can be proposed based on the connectional similarities. Indeed, a number of functional studies of the postrhinal cortex in the rat have appeared in the literature suggesting that the designation is a useful one (Bussey et al., 1998; Bucci et al., 2000; Myhrer, 2000; Naber et al., 2000; Vann et al., 2000).

Subdividing the perirhinal and postrhinal cortices

Areas 35 and 36 and the postrhinal cortices have not usually been subdivided because structural features tend to change in a gradient fashion such that cytoarchitectonically distinct subdivisions are difficult to identify. Because transitions between subregions are not usually abrupt, it could be argued that the further subdivision of areas 35, 36, and POR is unnecessary or superfluous. In the present study, with careful analysis of a number of cases and preparations, it was possible to reliably identify subregions of areas 35, 36 and POR on the basis of cytoarchitectonic and histochemical criteria. Moreover, subdividing these areas facilitated the careful description of the cytoarchitectural characteristics of the regions at all dorsoventral and rostrocaudal levels.

Perirhinal area 36 was parceled into three subregions, termed areas 36d, 36v, and 36p. Areas 36d and 36v occupy the rostral two-thirds of the region and are stacked one over the other in the dorsoventral plane. Area 36p occupies the caudal portion of the region. Although the cytoarchitecture is distinctly different between the subregions, the transitions are not sharply delineated. There were also cytoarchitectonic changes along the rostrocaudal axis, but these changes occurred in a gradient fashion in the rostral two-thirds of the region. Area 36p was parceled out because it was no longer possible to identify dorsoventral differences in cytoarchitecture, nor can the caudal portion be assigned to areas 36d or 36v on the basis of structural characteristics.

Perirhinal area 35 was parceled into two subregions. The two long narrow strips of cortex were termed areas 35d and 35v and lie next to each other parallel with the rhinal sulcus. This is consistent with Lorente de No (1933), who subdivided area 35 into areas 35a and 35b on the basis of cytoarchitectonic criteria. Area 35v occupies approximately the ventral bank of the rhinal sulcus and area 35d, the fundus. Again, although the cytoarchitecture is distinctly different between the subregions, the transition is not sharply delineated. There is little rostrocaudal variation in the structure or connectivity of the region.

The postrhinal cortex was also divided into two regions, PORd and PORv. The rostroventral portion of the region,

PORv, although very small, is different cytoarchitectonically and histochemically from the remainder of the area. Recent findings suggest it may also differ connectionally (Pitkanen et al., 2000). Regardless of putative connectional differences, the description of PORv should prove useful in the identification of the POR/entorhinal border at rostral levels.

Confirmatory analysis

With the development of computer-assisted, automated data collection techniques and high-capacity electronic storage, it is now possible to collect large sets of neuroanatomical data. This is exemplified in a study conducted by Burwell and Amaral (1998a) in which numbers and densities of retrogradely labeled cells in the entire neocortex, approximately 30 cortical regions, were estimated for about 40 retrograde tracer injection sites. With the new technology available to neuroanatomists, it seems appropriate to exploit techniques developed in other disciplines for summarizing and extracting information from large multivariate sets of neuroanatomical data, such as statistical classification techniques (Gordon, 1999). Large data sets are difficult to comprehend and interpret, but classification and clustering algorithms can be used to elucidate complex relationships among a set of objects. In the present context, cluster analysis, an external cluster validation technique, and canonical discriminant analysis were used to investigate the relationship of cortical afferentation to cortical regions defined by using traditional descriptive neuroanatomical techniques.

The cluster analysis of cortical afferent data included only those injection sites that were located in the regions of interest in order to examine the extent to which areas 35, 36, and POR can be differentiated from each other on the basis of cortical afferentation. The four clusters roughly approximated the neuroanatomical regions of area 35, ventral area 36, dorsal area 36, and the postrhinal cortex. This result is consistent with previous reports about the connectivity of this region (Romanski and LeDoux, 1993; Burwell and Amaral, 1998a,b). There is a dorsoventral cascade of connections in the perirhinal cortex, with dorsal area 36 receiving quantitatively more polymodal cortical input than ventral area 36 and ventral area 36 receiving more than area 35. Intrinsically, dorsal area 36 projects to ventral area 36 and ventral area 36 projects to area 35. The discriminant function analysis is also consistent with this pattern of connections in that the cluster comparable to dorsal area 36 is more closely connected with dorsally adjacent neocortical regions. In terms of the entorhinal projection, area 35 projects there most heavily, followed by ventral area 36, and then by dorsal area 36. The discriminant function analysis is also consistent with prior connectional results in that it suggests that area 35 is more closely connected with Entl than areas 36v and 36d.

Despite the limitations of these classification techniques, it was possible to provide confirmation of regional definitions based on structural analysis by using a dataset of retrogradely labeled cells that did not contain direct information about the location of the originating retrograde injection sites. This suggests that classification and clustering techniques can have broad applications in the study of brain function.

Comparison with prior studies

The border between the perirhinal and insular cortices. Rose (1928) conducted a thorough structural analysis of the insular cortex of humans and a number of other animals including the bat, hedgehog, mouse, squirrel, true hare, lemur, and baboon. The insular cortex was defined as seven-layered cortex with layers VI and VII corresponding to VIa and VIb in modern terminology. In all animals examined, the claustrum lay beneath the overlying layers of insular cortex. In the hare, lemur, baboon, and human, the insular cortex and claustrum were observed to be separated by the white matter of the capsule extrema. Rose noted that in the mouse, bat, and hedgehog, the claustrum still develops closely with the insular cortex, but the extreme capsule is absent. Nevertheless, he observed that even in the brains of these animals the claustrum is clearly separated from the overlying cortex and can be distinguished by its large cells as well as other cytoarchitectonic features. Thus, based on detailed cytoarchitectonic analyses in humans and other animals, Rose (1928) defined the insular region as the seven-layered cortex overlying the claustrum. Although this classic study did not include an analysis of insular cortex in the rat, all subsequent cytoarchitectonic analyses in that species have identified claustral cortex. Indeed, a recent comparative analysis suggested that the claustrum of rats is similar in shape, degree of differentiation, and size relative to isocortex and allocortex compared with other rodents (Kowianski et al., 1999). Moreover, phylogenetically, there is no reason to assert that insular cortex in the rat has extended beyond the boundaries established in more highly developed mammalian brains. Thus, the present results are consistent with Rose's findings in other species (Fig. 1A).

Following Rose's seminal studies (1928, 1929), a full description of the architecture and topography of cortical areas in the rat brain was not forthcoming for another decade and a half, with the appearance of the important studies of Krieg (1946a,b; 1947). Krieg agreed with Rose (1928) that "the extent of the claustrum coincides with the insula in man" (Krieg, 1946b). For the borders of the rat insular cortex, however, Krieg (1946a) stated that the use of the extent of the claustrum "though a convenient criteria, is a specious one." Instead, he designated the middle two quarters of the cortex around the rhinal sulcus as ventral agranular insular cortex. For reference, the caudal limit of the claustrum is located between these two quarters, at about the halfway point of the rhinal sulcus. Thus, the caudal border was placed several millimeters posterior to the caudal limit of the claustrum (Fig. 1B). Krieg provided no clear explanation for moving this border even in his own cytoarchitectonic description. Indeed, the insular cortex rostral to the caudal half of the rhinal sulcus is described as distinctly different from the caudally adjacent cortex: "As the caudal half of the rhinal sulcus begins, a new pattern is formed. The three-layered appearance of the cortex is lost altogether" (Krieg, 1946b). This change in the appearance of the cortex coincides with the caudal limit of the claustrum and with the cytoarchitectonic analysis in the present study (Fig. 5). Thus, Krieg's structural description, if not his terminology, is consistent with placing a regional border at the caudal limit of the claustrum.

Krettek and Price (1977a) provided a detailed description of the cytoarchitectonic features of granular and

agranular insular cortex as well as gustatory insular cortex. The definition of these regions in the rat, which was based on thalamic connectivity, conforms approximately to that of Rose (1928) and not to Krieg's (1946a). Other investigators mapping the entire cortex of the rat brain have also tended to adhere to the classical definition of insular cortex as overlying the claustrum (Fig. 1C) (Paxinos and Watson, 1986, 1998; Schober, 1986; Swanson, 1998). An exception to the trend resulted from Zilles' (1985) optical density analyses of cell- and fiber-stained preparations, which placed the insular-perirhinal border approximately 2 mm caudal to the end of the claustrum at -4.80 mm relative to bregma. It may be, however, that regional definitions based solely on optical density analyses of cortical structure are less reliable than analyses that also take into account other cortical features. For example, based on the same technique, Zilles placed the rostral entorhinal cortex border at -4.80 mm relative to bregma, a border that is not consistent with the topography of the origin of the entorhinal perforant pathway projection to the dentate gyrus (Dolorfo and Amaral, 1998) or recent structural descriptions of the entorhinal cortex, i.e., the ectopic layer II cells marking the border between lateral entorhinal cortex and area 35 (Insausti et al., 1997).

Investigators focusing primarily on the neuroanatomy of perirhinal cortex in the rat have tended to use the classical definition of insular cortex as coextensive with the claustrum (Krettek and Price, 1974; McIntyre et al., 1996; Burwell and Amaral, 1998b; Naber et al., 1999; Pitkanen et al., 2000; but see Deacon et al., 1983; Shi and Cassell, 1999). In contrast, borders used for direct neuroanatomical investigation of the rat insular cortex have tended to vary. Some reports define insular cortex as coextensive with the claustrum (Krettek and Price, 1977a; Saper, 1982; Kosar et al., 1986; McDonald and Jackson, 1987; Allen et al., 1991; Nakashima et al., 2000), whereas other reports place the perirhinal-insular border variously at more caudal locations (Fabri and Burton, 1991; McDonald, 1998; Shi and Cassell, 1998, 1999).

In the parcellation of Fabri and Burton (1991), the anterior perirhinal/posterior insular region in question was termed parietal rhinal cortex based on the pattern of labeling resulting from retrograde injections in somatosensory cortex. Label observed in this region was irregularly present and exhibited no topographical organization. McDonald (1998) later reported findings based on a series of anterograde injections in somatosensory cortex and the resulting label in the ventrally adjacent parietal ventral, parietal rhinal, and caudal agranular insular cortices, stating that the somatosensory insular cortex extends as far caudally as 3.5 mm posterior to bregma. Whereas these studies can provide useful information about the connectivity of somatosensory cortex, retrograde tracer injections in the region in question, i.e., anterior area 36, provide the most relevant data to address the issue of whether anterior area 36 itself is an ancillary somatosensory region. If the region in question is somatosensory cortex, then retrograde tracers in the region should produce a preponderance of label in primary somatosensory regions. If the region is polymodal or higher order associational cortex, the retrograde tracers should produce label in multiple sensory associational regions as well as other higher order associational regions.

Using retrograde tract tracing techniques, Burwell and Amaral (1998a) found the perirhinal cortex, including the area in question, to be polymodal in character. Perirhinal cortex receives its predominant cortical input from higher order polymodal association areas. As indicated in Figure 12C, less than one-third of its input arises from unimodal or unimodal associational areas. Figure 12 further shows that all rostrocaudal locations of area 36 can receive input from multiple sensory areas including visual areas. This finding is partially consistent with those of McDonald and Mascagni (1996), who reported, based on anterograde injections in occipital cortex, that input from occipital regions was limited to rostral area 36 from -3.3 to -3.8 mm relative to bregma. It is unclear why that study failed to show projections to more caudal parts of area 36.

To summarize, all parts of the perirhinal areas 36 and 35 receive polymodal and unimodal associational input. The unimodal input is from multiple sensory areas. In no case shown in Figure 12C did labeled cells in somatosensory cortex account for the majority of labeled cells, nor is visual input restricted to rostral area 36. Interestingly, a case from a prior report situated just rostral to area 36 or on the border of AIP and area 36 (119FB, Fig. 6, Burwell and Amaral, 1998a) also receives predominant input from polymodal associational regions. Only 41% of the total labeled cells were observed in unimodal regions: 18% percent in SSp or SSs, 11% in auditory regions, 7% in olfactory cortex, 3% in visual cortex, and 2% in gustatory regions. That case may be partially in rostral area 36, however, as its intrinsic connections extend throughout perirhinal cortex (Figure 3, Burwell and Amaral, 1998b).

Characterization of anterior perirhinal area 36 as polymodal association cortex is consistent with the findings of Guldin and Markowitsch (1983). Although they placed the perirhinal-insular border much more rostrally than the present report, those investigators also found evidence that the region in question, i.e., the anterior perirhinal cortex, is polymodal in character. They divided insular cortex into three components. Two of them, prefrontal insular and gustatory insular cortices, were consistent with Krettek and Price (1977a). They extended insular cortex caudally to include the anterior portion of the perirhinal cortical areas 35 and 36. This region they termed associative insular cortex based on its polymodal cortical input. Additionally, the region received thalamic input from supragenulate and medial geniculate nuclei, suggesting roles in both visual and auditory functions. Taken together, these findings contradict the notion that anterior perirhinal cortex is an ancillary somatosensory area. Thus, the weight of the evidence indicates that the anterior area 36, like the remainder of perirhinal cortex, is polymodal in character.

Shi and Cassell (1999) have suggested that the pattern of intrinsic perirhinal connections supports insular cortex as extending as far caudally as -4.0 mm relative to bregma. In a review, McDonald (1998) noted some unpublished data suggesting that the density of anterograde label falls off sharply at -3.8 mm relative to bregma, although light label continues for another 0.5 mm rostrally. Burwell and Amaral (1998b), however, showed that perirhinal intrinsic connections extend farther forward; anterograde or retrograde injections anywhere in the perirhinal cortex usually (13 of 17 injections) resulted in extensive labeling throughout the rostrocaudal extent of perirhinal cortex usually falling off between -2.45 and

-2.80 mm relative to bregma. The smaller injections (4 of 17) produced light or, in one case, no label between -2.5 and -3.0 mm.

It has been argued that the amygdala connections change between rostral and mid-rostrocaudal levels of the perirhinal cortex and that this change could signify a cortical border. McDonald (1998) suggested that the amygdalar perirhinal projections change dramatically at about -3.5 relative to bregma. Pikkariinen and Pitkanen (in press), in a comprehensive analysis of amygdala projections to the perirhinal and postrhinal cortices, show that input from four subnuclei (the intermediate and magnocellular divisions of basal nucleus and the parvicellular and magnocellular divisions of the accessory basal nucleus) appear to change at -4.16 mm relative to bregma in both area 36 and area 35. However, the projections from the remaining five subnuclei (the basal parvicellular nucleus, the accessory basal magnocellular nucleus, and the three subdivisions of the lateral nucleus) are not defined by changes in the projections at -4.16 mm, rather, those projections show a graded topography of terminations along the rostrocaudal extent of the perirhinal areas 35 and 36.

The exact placement of the caudal limit of the claustrum itself varies among investigators. For example, Paxinos and Watson (1998) show the claustrum ending at -1.88 mm relative to bregma at the level at which the lateral division of the amygdala is just beginning to appear. In a differing account, Swanson (1998) has the claustrum still visible at -2.45 mm relative to bregma, at a level at which the lateral division of the amygdala is well established. It may be that strain differences account for some of the discrepancy. For example, in Long-Evans hooded rats, the claustrum is not as easily distinguished from the overlying cortex (Burwell, unpublished observations). It is also possible that investigators apply different criteria to identify the caudal limit of the claustrum. In most animals, the ball of claustral cells identifiable at about -1.40 mm relative to bregma flattens before disappearing entirely. In the present account the caudal limit of the claustrum is identified as the point at which claustral cells are no longer visible. This is consistent with changes in layer V that differentiate insular regions from perirhinal regions. Taken together, cytoarchitectonic and connectional evidence confirms placement of the insular-area 36 border no farther caudal than -2.80 mm relative to bregma and the insular-area 35 border between -2.45 and -2.80 mm relative to bregma.

The border between the perirhinal and postrhinal cortices. The placement of the border between the perirhinal cortex and the postrhinal cortex is also worthy of discussion. The border generally appears at about -7.80 mm relative to bregma and is usually well marked by the presence of ectopic layer II cells in postrhinal cortex. The caudal limit of the angular bundle is a useful landmark as it almost always corresponds to the perirhinal-postrhinal border. The border is confirmed by connectional criteria including intrinsic connectivity and cortical input. Injections placed anywhere in the postrhinal cortex result in heavy label throughout the entire region that falls off dramatically at the borders (Burwell and Amaral, 1998b). Moreover, as shown by both cluster analyses, the patterns of cortical labeling resulting from injections anywhere in postrhinal cortex are highly intercorrelated and clearly differentiated from patterns result-

ing from sites in caudal area 36, which are also highly intercorrelated.

The postrhinal cortex receives cortical input that is very different from that of the perirhinal cortex (Burwell and Amaral, 1998a). The rostral limit of the postrhinal cortex corresponds to differences in cortical afferentation of the perirhinal cortex and the caudally adjacent postrhinal cortex. Compared with the caudal perirhinal cortex, the postrhinal cortex receives proportionally three times as much input from cingulate/retrosplenial areas, twice as much from posterior parietal cortex, and twice as much from visual association regions (Burwell and Amaral, 1998a). This is consistent with the cluster analysis in which two cases, on either side of the perirhinal/postrhinal border (120DY and 102FB in Fig. 12A) were included in different clusters. Regarding the projection to entorhinal cortex, the perirhinal/postrhinal border is distinguished by the projection to the medial limit of the lateral band of the Entm (Case 124DY, Burwell and Amaral, 1998b), which receives substantial input from the postrhinal cortex and none from the perirhinal cortex. The two regions are also distinguished by thalamic input. For example, POR, but not PER, receives input from the lateral posterior nucleus of the thalamus (Deacon et al., 1983; Burwell et al., 1995; Chen and Burwell, 1996; Shi and Cassell, 1997).

The dorsal borders. Historically, the dorsal borders of the perirhinal and postrhinal cortices have varied from definition to definition. Here, with a combination of markers for heavy metals, Nissl material, myelin, and acetylcholinesterase, it was possible to describe borders that could then be assessed with connectional findings from prior studies using similar borders (Burwell and Amaral, 1998a,b). Injection sites on either side of the dorsal borders of the perirhinal and postrhinal cortices at several rostrocaudal locations provided evidence consistent with the present definitions. The area 36 border with the dorsally adjacent region is largely consistent with Swanson's (1998) definition of the Te_v , but does tend to encroach upon Te_v especially at levels at which the substantia nigra is located (-4.45 mm to -6.65 mm relative to bregma). The border is consistent with prior descriptions of corticocortical connectivity including (1) the distinctions between cortical afferentation of area 36 and Te_v , and (2) the patterns of connectivity with the entorhinal cortex.

At rostral levels, direct comparisons of labeling resulting from retrograde injection sites in layers III-V on either side of the border between dorsal area 36 and Te_v indicate that there are dramatic differences in cortical afferentation (Fig. 6; Cases 120FB and 109FB, Burwell and Amaral, 1998a). This is well illustrated by differences in input from somatosensory areas. Te_v receives substantially more input from somatosensory and motor areas, e.g., Te_v at this rostrocaudal level receives more than one-fourth of its input from SSp (S1 according to Paxinos and Watson [1998]). In contrast, the ventrally adjacent portion of area 36 receives less than 1% of its total input from the same region. In contrast, area 36 compared with Te_v receives more than twice the proportion of input from posterior parietal cortex. Interestingly, even this rostral location in area 36 receives a substantial input from visual association cortices (more than 8%), whereas few if any cells were labeled in visual association cortex as a result of the Te_v injection site. Thus, it appears that area 36 is more polymodal in character than Te_v is at this level. Indeed,

Figure 12C provides good evidence of the polymodal character of all of the perirhinal cortex. Areas 36 and 35 receive less than one-third of their input from multiple unimodal associational regions, and the remaining input arises largely in higher order associational regions.

At mid-rostrocaudal levels of perirhinal cortex, it was also possible to make direct comparisons of labeling resulting from retrograde injection sites in superficial layers located on either side of the border between dorsal area 36 and ventral Te_v (Fig. 6, Cases 132DY and 122FB, Burwell and Amaral, 1998a). Again, there are striking differences in cortical afferentation. Te_v at this level receives more input from somatosensory cortex than area 36 does (about 10% compared with less than 1%). Te_v at this level also receives more input from auditory cortex than area 36 does (about 30% compared with 16%).

Analysis of cortical input to the entorhinal cortex (Burwell and Amaral, 1998a) provided additional connectional criteria for establishing the Te_v /Area 36 border. The Entl receives the large majority of its perirhinal input from area 35. Substantial input, however, also originates in area 36, but not from Te_v . In a previous study, the density of labeled cells in area 36 following injection of retrograde tracer in the Entl was four times the density in Te_v in the same experimental cases (Burwell and Amaral, 1998a).

Regarding the postrhinal cortex, the dorsal border at rostral levels cuts deeply into a portion of Te_v as defined by Swanson (1998) and TeA as defined by Paxinos and Watson (1998). The dorsal border described here for more caudal levels of postrhinal cortex approximates the one with Te_v (Swanson, 1998) but encroaches upon TeA (Paxinos and Watson, 1998) and TE2 (Zilles, 1985).

The border between the postrhinal cortex and the dorsally adjacent temporal region is also informed by cortical afferentation. Compared with a control injection, the postrhinal cortex receives substantially more input from frontal, insular, and cingulate cortices, and substantially less from primary visual cortex (Fig. 6, Case 94DY in Burwell and Amaral, 1998a). Thus, the dorsal border of postrhinal cortex as defined is consistent with connectional criteria showing that the postrhinal cortex is more polymodal in character compared with the dorsally adjacent region, which can best be described as visual association cortex. The postrhinal intrinsic connections were also useful in defining the dorsal border because an injection anywhere in the region results in dense label falling off sharply at the borders (see particularly Figs. 8H and 11I, Burwell and Amaral, 1998a).

Comparisons with monkey studies

In the monkey brain, as in the rat brain, the spatial arrangements of the perirhinal, postrhinal/parahippocampal, and entorhinal cortices and their boundaries with adjacent cortical regions are remarkably similar (Burwell, 2000). Although difficult to ascertain because of the gyrencephalic character of the monkey cortex, the juxtaposition of the perirhinal cortex with agranular insular cortex is also similar (Jones and Burton, 1976). In the lissencephalic rat brain, agranular insular cortex (AIP) is juxtaposed to the perirhinal areas 36 and 35. In the monkey brain, area 36c and parts of area 36r are ventrally positioned. Area 36r rises upward over the lateral part of the temporal pole and becomes area 36d, which continues backward toward the lateral sulcus. Area TG of the temporal pole is located medially to area 36d. As the cortex associated with the rhinal sulcus enters into

the lateral sulcus, it becomes insular cortex. Thus, in the monkey as in the rat, agranular insular areas border the perirhinal cortex.

The regions in the monkey brain that correspond to PER and POR, the perirhinal and parahippocampal cortices, respectively, are much more clearly differentiated cytoarchitecturally. Thus it is challenging to draw cross-species comparisons based on structure alone. Nevertheless, it is possible to identify for the perirhinal cortex certain signature features in the rat brain that are also present in the monkey brain (Suzuki, personal communication). In both species, area 35 is more poorly laminated than area 36, with area 35 completely lacking a granular layer. Area 35 has a broader layer I than the adjacent area 36. Layers II and III of area 35 are difficult to distinguish from one another compared with area 36. The packing density of layer V cells is higher in area 35 than in area 36. In both species, large darkly stained pyramidal cells in layer V characterize areas 35 and 36. Layer VI is narrower in area 35 than area 36. Area 36 in both the monkey and the rat is more granular than area 35, although in the rat area 36 must be described as dysgranular at best. Also, in both, layer II of area 36 is characterized by aggregates of cells, giving the layer an irregular or patchy appearance. In addition to these structural similarities, the rat and monkey perirhinal regions exhibit similarities in cortical and subcortical connectivity (reviewed in Burwell et al., 1995, 1996; Burwell, 2000).

The rat postrhinal cortex and the monkey parahippocampal cortices exhibit few convincing structural similarities. Perhaps the best that can be said is that, in both species, the region is more granular laterally than medially (dorsally vs. ventrally in the rat). As described earlier, available evidence reveals substantial homology of the cortical afferentation of the rat postrhinal and monkey parahippocampal cortices. Both receive substantial visual association and visuospatial input from cortical and subcortical sources (Burwell et al., 1995). Additionally, the parahippocampal cortex of the monkey receives input from the pulvinar (Baleydier and Mauguire, 1985), which may be the homologue of the rat lateral posterior nucleus of the thalamus (Takahashi, 1985), a nucleus that is interconnected with the rat postrhinal cortex (Deacon et al., 1983; Burwell et al., 1995; Chen and Burwell, 1996; Shi and Cassell, 1997). There are also similarities in the connections with the amygdala. For example, the monkey parahippocampal cortex projects to the lateral nucleus of the amygdala, but less strongly than the perirhinal cortex (Stefanacci and Amaral, 2000). A similar situation exists in the rat (reviewed in Pitkanen et al., 2000).

Thus, it can be stated that, between the monkey and rat perirhinal cortex, structural and connectional homology are both evident, whereas between the monkey parahippocampal cortex and the rat postrhinal cortex, connectional homology is more evident.

CONCLUSIONS

This definition of the perirhinal and postrhinal cortices is based on careful analysis of cytoarchitecture, myeloarchitecture, histochemistry, and the available connectional data. The description of the cytoarchitecture of these regions will facilitate addressing the many questions about the perirhinal and postrhinal cortices that are outstanding. For example, what are the fundamental operations

performed by each of these regions upon sensory associational input? How do they interact with each other and with other memory-related brain regions? Are they preferentially involved in memory, or are there other cognitive functions to which they contribute? It is hoped that this definition of boundaries accompanied by the careful documentation of structural characteristics of these regions will contribute to ongoing research on the functions of the cortical regions surrounding the hippocampus.

ACKNOWLEDGMENTS

The author acknowledges Guadalupe Garcia for her excellent technical assistance and David G. Amaral, Perika Deroche, Michela Gallagher, Asla Pitkanen, Peter R. Rapp, Larry W. Swanson, Menno P. Witter, and Wendy A. Suzuki for reading and commenting on portions of this manuscript.

LITERATURE CITED

- Aggleton JP, Brown MW. 1999. Episodic memory, amnesia, and the hippocampal-anterior thalamic axis. *Behav Brain Sci* 22:425–489.
- Aggleton JP, Keen S, Warburton EC, Bussey TJ. 1997. Extensive cytotoxic lesions involving both the rhinal cortices and area TE impair recognition but spare spatial alternation in the rat. *Brain Res Bull* 43:279–287.
- Allen GV, Saper CB, Hurley KM, Cecheto DF. 1991. Organization of visceral and limbic connections in the insular cortex of the rat. *J Comp Neurol* 311:1–16.
- Baleydier C, Mauguire F. 1985. Anatomical evidence for medial pulvinar connections with the posterior cingulate cortex, the retrosplenial area, and the posterior parahippocampal gyrus in monkeys. *J Comp Neurol* 232:219–228.
- Brodmann K. 1909. Vergleichende Lokalisationslehre der Grosshirnrinde in ihren Prinzipien dargestellt auf Grund des Zellenbaues. Leipzig: Barth.
- Bucci DJ, Phillips RG, Burwell RD. 2000. Contributions of postrhinal and perirhinal cortex to contextual information processing. *Behav Neurosci* 114:882–894.
- Burwell RD. 2000. The parahippocampal region: corticocortical connectivity. *Ann NY Acad Sci* 911:25–42.
- Burwell RD, Amaral DG. 1998a. Cortical afferents of the perirhinal, postrhinal, and entorhinal cortices. *J Comp Neurol* 398:179–205.
- Burwell RD, Amaral DG. 1998b. The perirhinal and postrhinal cortices of the rat: interconnectivity and connections with the entorhinal cortex. *J Comp Neurol* 391:293–321.
- Burwell RD, Witter MP, Amaral DG. 1995. The perirhinal and postrhinal cortices of the rat: a review of the neuroanatomical literature and comparison with findings from the monkey brain. *Hippocampus* 5:390–408.
- Burwell RD, Suzuki WA, Insausti R, Amaral DG. 1996. Some observations on the perirhinal and parahippocampal cortices in the rat, monkey, and human brains. In: Ono T, editor. Perception, memory, and emotion: frontier in neuroscience. New York: Elsevier. p 95–110.
- Bussey TJ, Muir JL, Aggleton JP. 1998. Functionally dissociating aspects of event memory: the effects of combined perirhinal and postrhinal cortex lesions on object and place memory in the rat. *J Neurosci* 19:495–502.
- Chen H-C, Burwell RD. 1996. An anterograde tract-tracing study of the perirhinal and postrhinal cortical projections to the thalamus in the rat brain. *J Undergrad Res* 3:47–68.
- Deacon TW, Eichenbaum H, Rosenberg P, Eckmann KW. 1983. Afferent connections of the perirhinal cortex in the rat. *J Comp Neurol* 220:168–190.
- Dolorfo CL, Amaral DG. 1998. The entorhinal cortex of the rat: topographic organization of the cells of origin of the perforant path projection to the dentate gyrus. *J Comp Neurol* 398:25–48.
- Fabri M, Burton H. 1991. Ipsilateral cortical connections of primary somatic sensory cortex in rats. *J Comp Neurol* 311:405–424.
- Gordon AD. 1999. Classification. London: Chapman & Hall/CRC.

- Guidin WO, Markowitsch HJ. 1983. Cortical and thalamic afferent connections of the insular and adjacent cortex of the rat. *J Comp Neurol* 215:135–153.
- Hedreen JC, Bacon SJ, Price DL. 1985. High resolution histochemical techniques for acetylcholinesterase-containing axons. *J Histochem Cytochem* 33:134–140.
- Hubert L, Arabie P. 1986. Comparing partitions. *J Classification* 2:193–218.
- Insausti R, Amaral DG, Cowan MW. 1987. The entorhinal cortex of the monkey: II. Cortical afferents. *J Comp Neurol* 264:356–395.
- Insausti R, Herrero MT, Witter MP. 1997. Entorhinal cortex of the rat: cytoarchitectonic subdivisions and the origin and distribution of cortical efferents. *Hippocampus* 7:146–183.
- Jones EG, Burton H. 1976. Areal differences in the laminar distribution of thalamic afferents in cortical fields of the insular, parietal and temporal regions of primates. *J Comp Neurol* 168:197–248.
- Kosar E, Grill HJ, Norgren R. 1986. Gustatory cortex in the rat. I. Physiological properties and cytoarchitecture. *Brain Res* 379:329–341.
- Kosel KC. 1981. The anatomical organization of the parahippocampal cortices (areas 28 and 35) in the rat. In: *Anatomy*. Iowa City: University of Iowa. p 387.
- Kowianski P, Dziewiatkowski J, Kowianska J, Morys J. 1999. Comparative anatomy of the claustrum in selected species: a morphometric analysis. *Brain Behav Evol* 53:44–54.
- Krettek JE, Price JL. 1974. Projections from the amygdala to the perirhinal and entorhinal cortices and the subiculum. *Brain Res* 71:150–154.
- Krettek JE, Price JL. 1977a. The cortical projections of the mediodorsal nucleus and adjacent thalamic nuclei in the rat. *J Comp Neurol* 171:157–192.
- Krettek JE, Price JL. 1977b. Projections from the amygdaloid complex to the cerebral cortex and thalamus in the rat and cat. *J Comp Neurol* 172:687–722.
- Krieg WJS. 1946a. Connections of the cerebral cortex. I. The albino rat. A. Topography of the cortical areas. *J Comp Neurol* 84:221–275.
- Krieg WJS. 1946b. Connections of the cerebral cortex. I. The albino rat. B. Structure of the cortical areas. *J Comp Neurol* 84:277–323.
- Krieg WJS. 1947. Connections of the cerebral cortex. I. The albino rat. C. Extrinsic connections. *J Comp Neurol* 86:267–394.
- Liu P, Bilkey D. 1998. Perirhinal cortex contributions to performance in the Morris water maze. *Behav Neurosci* 112:304–315.
- Lorente de No R. 1933. Studies on the structure of the cerebral cortex. I. *Area entorhinalis*. *J Psychol Neurol* 45:113–177.
- McDonald AJ. 1998. Cortical pathways to the mammalian amygdala. *Prog Neurobiol* 55:257–332.
- McDonald AJ, Jackson TR. 1987. Amygdaloid connections with posterior insular and temporal cortical areas in the rat. *J Comp Neurol* 262:59–77.
- McDonald AJ, Mascagni F. 1996. Cortico-cortical and cortico-amygdaloid projections of the rat occipital cortex: a *Phaseolus vulgaris* leucoagglutinin study. *Neurosci* 71:37–54.
- McIntyre DC, Kelly ME, Staines WA. 1996. Efferent projections of the anterior perirhinal cortex in the rat. *J Comp Neurol* 369:302–318.
- Moga MM, Weis RP, Moore RY. 1995. Efferent projections of the paraventricular thalamic nucleus in the rat. *J Comp Neurol* 359:221–238.
- Myhrer T. 2000. Effects of selective perirhinal and postrhinal lesions on acquisition and retention of a visual discrimination task in rats. *Neurobiol Learn Mem* 73:68–78.
- Naber PA, Witter MP, Lopez da Silva FH. 1999. Perirhinal cortex input to the hippocampus in the rat: evidence for parallel pathways, both direct and indirect. A combined physiological and anatomical study. *Eur J Neurosci* 11:4119–4133.
- Naber PA, Witter MP, Lopes da Silva FH. 2000. Differential distribution of barrel or visual cortex. Evoked responses along the rostro-caudal axis of the peri- and postrhinal cortices. *Brain Res* 877:298–305.
- Naber R. 1999. The hippocampal memory system: functional analysis of parallel pathways through the subiculum. Wageningen, The Netherlands: Ponsen & Looijen.
- Nakashima M, Uemura M, Yasui K, Ozaki HS, Tabata S, Taen A. 2000. An anterograde and retrograde tract-tracing study on the projections from the thalamic gustatory area in the rat: distribution of neurons projecting to the insular cortex and amygdaloid complex. *Neurosci Res* 36:297–309.
- Otto T, Wolf D, Walsh TJ. 1997. Combined lesions of perirhinal and entorhinal cortex impair rat's performance in two versions of the spatially guided radial-arm maze. *Neurobiol Learning Memory* 68:21–31.
- Paxinos G, Watson C. 1986. The rat brain in stereotaxic coordinates. 2nd edition. San Diego: Academic Press.
- Paxinos G, Watson C. 1998. The rat brain in stereotaxic coordinates. 4th edition. San Diego: Academic Press.
- Pikkarainen M, Pitkanen A. in press. Projections from the lateral, basal, and accessory basal nuclei of the amygdala to the perirhinal and postrhinal cortices in rat. *Cereb Cortex*.
- Pitkanen A, Pikkarainen M, Nurminen N, Ylinen A. 2000. Reciprocal connections between the amygdala and the hippocampal formation, perirhinal cortex, and postrhinal cortex in rat. A review. *Ann NY Acad Sci* 911:369–391.
- Quinn B, Graybiel AM. 1994. Myeloarchitectonics of the primate caudate-putamen. In: Percheron G, McKenzie JS, Férgér J, editors. *The basal ganglia IV: new ideas and data on structure and function*. New York: Plenum Press. p 35–41.
- Rand WM. 1971. Objective criteria for the evaluation of clustering methods. *J Am Stat Assoc* 66:846–850.
- Romanski LM, LeDoux JE. 1993. Information cascade from primary auditory cortex to the amygdala: cortico-cortical and cortico-amygdaloid projections of temporal cortex in the rat. *Cereb Cortex* 3:515–532.
- Rose M. 1928. Die Inselrinde des Menschen und der Tiere. *J Psychol Neurol* 37:467–624.
- Rose M. 1929. Cytoarchitektonischer atlas der Groshirnrinde der Maus. *J Psychol Neurol* 40:1–32.
- Rudiger L. 1999. Organization of projections to temporal cortex originating in the thalamic posterior intralaminar nucleus of the rat. *Exp Brain Res* 127:314–320.
- Saper CB. 1982. Convergence of autonomic and limbic connections in the insular cortex of the rat. *J Comp Neurol* 210:163–173.
- SAS. 1996. SAS software. Cary, NC: SAS Institute.
- Schmued LC. 1990. A rapid, sensitive histochemical stain for myelin in frozen brain sections. *J Histochem Cytochem* 38:717–720.
- Schober W. 1986. The rat cortex in stereotaxic coordinates. *J Hirnforschung* 27:121–143.
- Shammah-Lagnado SJ, Alheid GF, Heimer L. 1999. Afferent connections of the interstitial nucleus of the posterior limb of the anterior commissure and adjacent amygdalostriatal transition area in the rat. *Neuroscience* 94:1097–1123.
- Shi CJ, Cassell MD. 1997. Cortical, thalamic, and amygdaloid projections of rat temporal cortex. *J Comp Neurol* 382:153–175.
- Shi CJ, Cassell MD. 1998. Cascade projections from somatosensory cortex to the rat basolateral amygdala via the parietal insular cortex. *J Comp Neurol* 399:469–491.
- Shi CJ, Cassell MD. 1999. Perirhinal cortex projections to the amygdaloid complex and hippocampal formation in the rat. *J Comp Neurol* 406:299–328.
- Slovitor RS. 1982. A simplified Timm stain procedure compatible with formaldehyde fixation and routine paraffin embedding of rat brain. *Brain Res*–Bull 8:771–774.
- Stefanacci L, Amaral DG. 2000. Topographic organization of cortical inputs to the lateral nucleus of the macaque monkey amygdala: a retrograde tracing study. *J Comp Neurol* 421:52–79.
- Suzuki WA. 1996. The anatomy, physiology, and functions of the perirhinal cortex. *Curr Opin Neurobiol* 6:179–186.
- Suzuki WA, Amaral DG. 1994a. The perirhinal and parahippocampal cortices of the Macaque monkey: cortical afferents. *J Comp Neurol* 350:497–533.
- Suzuki WA, Amaral DG. 1994b. Topographic organization of the reciprocal connections between the monkey entorhinal cortex and the perirhinal and parahippocampal cortices. *J Neurosci* 14:1856–1877.
- Swanson LW. 1992. Brain maps: structure of the rat brain. 2nd edition. Amsterdam: Elsevier.
- Swanson LW. 1998. Brain maps: structure of the rat brain. 2nd edition. Amsterdam: Elsevier.
- Takahashi T. 1985. The organization of the lateral thalamus of the hooded rat. *J Comp Neurol* 231:281–309.
- Van Groen T, Kadish I, Wyss JM. 1999. Efferent connections of the anteromedial nucleus of the thalamus of the rat. *Brain Res Brain Res Rev* 30:1–26.
- Van Hoesen GW. 1995. Anatomy of the medial temporal lobe. *Magn Reson Imaging* 13:1047–1055.

- Vann SD, Brown MW, Erichsen JT, Aggleton JP. 2000. Fos imaging reveals differential patterns of hippocampal and parahippocampal subfield activation in rats in response to different spatial memory tests. *J Neurosci* 20:2711–2718.
- Wada E, Wada K, Boulter J, Deneris E, Heinemann S, Patrick J, Swanson LW. 1989. Distribution of alpha 2, alpha 3, alpha 4, and beta 2 neuronal nicotinic receptor subunit mRNAs in the central nervous system: a hybridization histochemical study in the rat. *J Comp Neurol* 284:314–335.
- Wiig KA, Burwell RD. 1998. Memory impairment on a delayed-non-matching-to-position task following lesions of the perirhinal cortex in the rat. *Behav Neurosci* 112:828–838.
- Witter MP, Groenewegen HJ. 1984. Laminar origin and septotemporal distribution of entorhinal and perirhinal projections to the hippocampus in the cat. *J Comp Neurol* 224:371–385.
- Witter MP, Wouterlood FG, Naber PA, Van Haeften T. 2000. Anatomical organization of the parahippocampal-hippocampal network. *Ann NY Acad Sci* 911:1–24.
- Zhu XO, McCabe BJ, Aggleton JP, Brown MW. 1997. Differential activation of the rat hippocampus and perirhinal cortex by novel visual stimuli and a novel environment. *Neurosci Lett* 229:141–143.
- Zilles K. 1985. *The cortex of the rat: a stereotaxic atlas*. Berlin: Springer-Verlag.
- Zilles K. 1990. Anatomy of the neocortex: cytoarchitecture and myeloarchitecture. In: Kolb B, Tees RC, editors. *The cerebral cortex of the rat*. Cambridge, MA: MIT Press. p 77–112.